

AD-A278 094

Best Available Copy

FIFTH FINAL TECHNICAL REPORT

Title: "Optical Properties of Doped Sol-Gel Silica Glasses"

Principal Investigator: Professor Terence A. King

Contractor: University of Manchester

Contract Number: DAJA 45-02-C-0009

Report Period: 07/06/93 - 12/31/93

5680 94-11041

DTIC  
ELECTE  
APR 12 1994

UNIVERSITY OF MANCHESTER  
PHYSICAL LABORATORIES

MANCHESTER ENGLAND

DTIC QUALITY INSPECTED 3

94 4 11 180

**Best  
Available  
Copy**

# FIFTH FINAL TECHNICAL REPORT

Title: "Optical Properties of Doped Sol-Gel Silica Glasses"

Principal Investigator: Professor Terence A King

Contractor: University of Manchester

Contract Number: DAJA 45-92-C-0005

Report Period: 07/06/93 - 12/31/93

The report in this document has been made possible through the support and sponsorship of the US Government through its European Research Office of the US Army. This report is intended for the internal management use of the contractor and the US Government.

Accession For	
NTIS CRA&I	<input checked="" type="checkbox"/>
DTIC TAB	<input type="checkbox"/>
Unannounced	<input type="checkbox"/>
Justification	
By	
Distribution /	
Availability Codes	
Dist	Avail and/or Special
A-1	

DTIC  
ELECTE  
APR 12 1994  
S G D

DTIC QUALITY INSPECTED 3



REPORT DOCUMENTATION PAGE			Form Approved GSA No. 0704-0100	
<small>Public reporting burden for this collection of information is estimated to average 1 hour per response, including the time for reviewing instructions, searching existing data sources, gathering and maintaining the data needed, and completing and reviewing the collection of information. Send comments regarding this burden estimate or any other aspect of this collection of information, including suggestions for reducing this burden, to Washington Headquarters Services, Directorate for Information Operations and Reports, 1215 Jefferson Davis Highway, Suite 1204, Arlington, VA 22202-4302, and to the Office of Management and Budget, Paperwork Reduction Project (0704-0100), Washington, DC 20503.</small>				
1. AGENCY USE ONLY (Leave blank)	2. REPORT DATE 01/04/94	3. REPORT TYPE AND DATES COVERED Final 06/07/93-12/31/93		
4. TITLE AND SUBTITLE Optical Properties of Doped Sol-Gel Silica Glasses		5. FUNDING NUMBERS DAJA 45-92-C-005 (WK2Q6C-6709-EE01)		
6. AUTHOR(S) T A King, G Gall, X Li and M Rahn				
7. PERFORMING ORGANIZATION NAME(S) AND ADDRESS(ES) University of Manchester Physics Department, Schuster Laboratory Manchester M13 9PL, UK		8. PERFORMING ORGANIZATION REPORT NUMBER		
9. SPONSORING/MONITORING AGENCY NAME(S) AND ADDRESS(ES)		10. SPONSORING/MONITORING AGENCY REPORT NUMBER		
11. SUPPLEMENTARY NOTES				
12a. DISTRIBUTION/AVAILABILITY STATEMENT Fiscal Officer, US Army Research Development and Standardization Group, UK		12b. DISTRIBUTION CODE		
13. ABSTRACT (Maximum 200 words)  Sol-gel optical composites have been developed and characterised for potential applications in optics, lasers, nonlinear optics and optoelectronics. Post-doped xerogels have been index matched by in-situ polymerisation of monomer to form inorganic-organic composites of low scatter and high optical quality. Characterisation of microstructure has been made by visible and IR absorption and Raman Spectroscopy and optical quality by attenuation and scatter measurement. Doping techniques have been optimised using hypercritical drying and vacuum impregnation, and doping distribution monitored by laser-induced fluorescence. One-tenth wavelength surfaces have been formed by novel optical polishing. Organic molecular dopants have been tested in laser and nonlinear systems. Initial third harmonic generation and 2-scan measurements have shown the potential for saturable absorption and optical limiting.				
14. SUBJECT TERMS		15. NUMBER OF PAGES 53		
		16. PRICE CODE		
17. SECURITY CLASSIFICATION OF REPORT	18. SECURITY CLASSIFICATION OF THIS PAGE	19. SECURITY CLASSIFICATION OF ABSTRACT	20. LIMITATION OF ABSTRACT	

NSN 7540-01-280-3500

Standard Form 298 (Rev. 2-89)  
Prescribed by ANSI Std. Z39-18  
298-102

**Contract: DAJA 45-92-C-005**

**Optical Properties of Doped Sol-Gel Silica Glasses**

**5th Final Technical Report: 06/07/93 - 12/31/93**

**1. Introduction**

This contract had the following objectives

- (a) Preparation of sol-gel composite materials
- (b) Determination of linear optical characteristics
- (c) Preparation and characterisation of nonlinear optical media

The preparation of the sol-gel composites has been based on the development of doping techniques of pre-formed sol-gel silica with organic materials. The post-doping method, in which the dopant is added to the porous sol-gel glass, is compared with pre-doping in which the optically active element is added with the initial starting materials in the sol. The incorporation of refractive index matching material, either as monomers for conversion to polymer or by back-filling with sol, has been developed to make samples of high optical quality.

The characterisation of the linear optical properties of the materials has included investigation of the microstructure of the material by several spectroscopic techniques and the characterisation of the spatial distribution of dopants by laser induced fluorescence. A detailed understanding of the nanocomposite material is valuable for optimisation of materials for optical applications.

The preparation and characterisation of nonlinear optical materials aims to provide the essential background for nonlinear applications. Two applications of particular interest are as optical limiters and as reverse saturable absorbers. The programme of fabrication and nonlinear optical characterisation has been directed towards these applications.

**2. Scientific Work Accomplished**

Within the contract period a wide range of achievements have been made in the objective areas described in section 1. A fuller description of details of the work is given in the Annex to this report and in the previous reports 1-4 detailed in section 3. A summary of the achievements is given below.

## 2.1 Sample preparation

Preparation of post-doped sol-gel glass with incorporation of active organic molecules has been progressed significantly. These have been used for laser and nonlinear optical applications. The distribution of dopant has been monitored in a technique of laser induced fluorescence which has been developed during this programme and described later.

The preparation of pre-doped samples has been used to prepare active material by addition of optically active compounds at the sol stage. A further pre-doping method in which organic elements are bound to the inorganic matrix to make ormosil (organically modified silica) has produced high quality optical material. These two methods of pre-doping provides homogeneous samples but the inorganic matrix has mechanical properties equivalent to the low temperature preparation, limited to  $< 200^{\circ}\text{C}$ , and has an operating temperature limit of about  $200^{\circ}\text{C}$ .

### (b) Index matching

The filling of the residual pore free volume remaining after doping in the post-doping technique has been accomplished, using back-filling with monomer followed by in-situ polymerisation, or by back-filling with sol and subsequent gellation. Filling the pore free volume with polymethyl methacrylate (PMMA) has produced high quality material with optical loss  $< 0.3 \text{ dB/cm}$  at  $633\text{nm}$ .

### (c) Optical polishing

Techniques have been established to optical polish porous sol-gel glass and back-filled material to optical quality finish. A computer controlled lapping and polishing system has been used in a technique in which the optical working materials have been optimised. These methods have been developed so that routine finishing to better than on-tenth of a wavelength can be achieved. The optically finished material provides samples of high optical quality for nonlinear and laser applications.

## 2.2 Microstructural characterisation

The microstructure of the inorganic-organic composites has been characterised using FTIR, uv/visible absorption, IR and near-IR absorption and NMR. The molecular weight of the polymer back-filling has been determined using GPC. The PMMA impregnated gel silica glass and the methyltrimethoxysilane (MTMS)/tetramethoxysilane (TMOS) derived ormosil have been characterised to determine the role of the organic compounds in the formation of the sol-gel structure and their effects on the properties of the materials.

In the sol-gel derived ormosil materials it is proposed that the methyl group has a chain-terminating effect and stops the formation of Si-O-Si siloxane bonds and acts as a network modifier rather than a network former. The incorporation of methyl groups in the network creates more open structures in the hybrid organic/inorganic MTMS/TMOS derived materials than that in the inorganic TMOS derived xerogels. The mobility and flexibility of the polymer in the sol-gel process are increased for the ormosil and leads to a high efficiency of polycondensation reactions by dehydroxylation of Si-OH groups. Formation of trisiloxane rings is favoured by the more open structure, while a number of the bridging Si-O-Si siloxane units are less than in the xerogel due to the substitution of non-condensable Si-CH<sub>3</sub> groups for Si-OH groups.

The xerogel material index matched with PMMA has interactions with the inorganic silica phase by hydrogen bonding between carbonyl and silanol groups and the interaction occurs mainly at the boundary of the two phases. The bulk properties of the two phases are in the main retained. The substrate with the more open structure and larger pore size facilitates the polymerisation.

### 2.3 Optical characterisation

Techniques have been established to measure the three-dimensional distribution of the dopant using laser induced fluorescence. Further techniques to characterise optical quality have been implemented using optical attenuation and optical scatter. Forward scattering of a narrow beam from a laser source has been used as a monitor of optical quality. The surface quality of samples prepared using the optical polishing described in section 1 has been measured using surface interferometry.

### 2.4 Development of tunable sol-gel glass lasers

One of the applications for the optically active sol-gel glass is a tunable solid-state laser. Aspects of this work are described in section 3 of the Annex.

The sol-gel glass lasers form a device for which the materials and optical quality directly influence the performance. The sol-gel medium offers the prospect of efficient, stable and tunable pulsed laser sources. In the studies described in this report laser efficiency and photostability are investigated.

### 2.5 Preparation and characterisation of sol-gel nonlinear optical media

The primary aim of the programme has been the development of media for nonlinear optical application, particularly for optical limiting and reverse saturable absorption. The work described in 2.1 - 2.3 are directly relevant to this application. Various doping techniques have been investigated and the dependence of the linear and nonlinear

optical characteristics on the preparation.

Two families of organic dyes have been used and impregnated into sol-gel glass matrices: dithiolene derivatives and metal phthalocyanine derivatives. Nonlinear optical measurements have been made using third harmonic generation and z-scan techniques. These initial measurements are described in section 4 of the Annex. Initial results from dithiolene derivatives have indicated similar  $\chi^4$  values to those obtained with polymer PMMA as a host. With chloro-phthalocyanine z-scan measurements shown characteristic features from which nonlinear optical coefficients are presently being obtained.

### 3. Personnel

The following personnel have been engaged on the project:

Principal investigator: Professor Terence A King  
Research Associates: Dr X Li  
Dr D West  
Graduate students: G Gall  
M. Rahn

### Reports

1. First Interim Report on Contract DAJA 45-92-C-005  
1 March 1992, period 01/01/91 - 02/20/92
2. Second Interim Report on Contract DAJA 45-92-C-005  
1 July 1992, Period 02/21/92 - 06/20/92
3. Third Interim Report on Contract DAJA 45-92-C-005  
1 January 1993, Period 06/12/92 - 12/20/92
4. Fourth Interim Report on Contract DAJA 45-92-C-005  
1 July 1993, Period 12/21/92 - 06/06/93



**Contract: DAJA 45-92-C-005**

**Optical Properties of Doped Sol-Gel Silica Glasses**

**5th Final Technical Report: 06/07/93 - 12/31/93**

**1. Introduction**

During the period of this contract over 1992-94 optical materials based on sol-gel processing have become of substantial interest. The fabrication by sol-gel methods enables low temperature production of optical materials with optical, mechanical, laser, nonlinear optical and quantum properties which can be tailored to applications. The materials and manufacturing methods have become sufficiently developed to produce optical elements such as active waveguides for integrated optics and optoelectronics. These methods show strong potential for large scale manufacture for monolith structures and using laser writing and laser embossing techniques for waveguides. Optical elements of directional couplers, lenses, gratings, interferometers, thin films, amplifiers and frequency doublers can be incorporated in structures which are compatible to compact, high density devices and fibre optic connection.

In the sol-gel process the room temperature hydrolysis of metal alkoxides forms metal oxides based on, for example, silica, titania or zirconia. Dissolving the metal alkoxide in alcohol with water leads to hydrolysis of the alkoxides to form the sol, this is a homogeneous distribution of molecular clusters or colloids in the alcohol solution. When formed into coatings, drawn into fibres or made in net cast shape the structure and interactions in the colloids determine the properties. The properties can be controlled by chemical means to tailor the properties for optical application. The interfacial structure and colloidal interactions determine the mechanical and optical properties of the materials.

The growth of a three-dimensional network as the colloids grow in the sol forms the gel having a metal oxide matrix. Heating of the gel over 150 to 600°C removes solvents from the gel and sinters the network with gel drying, shrinking, hardening and densifying and having a degree of porosity of 20-60%. Further increase in temperature up to 1200°C steadily reduces the porosity and leads to a fully dense glass at about 1200°C.

The shrinkage process requires careful control since it can lead to cracking. For thin films this makes the formation of films greater than 1µm thickness or the formation of macroscopic monoliths difficult. The process can be controlled by hypercritical drying and by the use of organic additives to relieve stresses in the inorganic matrix.

Hybrid materials, *ormocers*, can be produced by covalently bonding the organic additive and inorganic matrix. The sol can also be doped with organic dye molecules or with

optically active inorganics to form laser or nonlinear optical compounds. The refractive index of the materials can be varied by densification, by additives or by mixtures of inorganic starting material. Other elements such as semiconductor or metallic quantum dots can be incorporated.

An alternative to forming ormoer material is to pre-form bulk sol-gel glass monoliths or thin films by partial densification by raising the temperature to intermediate values. Then optical active elements may be added by diffusion into the porous matrix, where the optical element lodges on to the surfaces of the pores by hydrogen bonding and van der Waals forces. The residual free volume can be filled with other materials to remove refractive index discontinuities. These would lead to scattering. One method to remove the residual free volume is by impregnation with a monomer, with subsequent polymerisation, to form an inorganic matrix-polymer composite. This method has been shown in this contract to lead to monolithic samples of high optical quality. Photopolymerisation of added compounds can be used to form surface layers which prevent the ingress of moisture or to be used to laser write waveguides or gratings. These types of hybrid structures have only in recent years been studied and they have great potential for future applications.

The sol-gel glasses and the inorganic-organic composites are at an early stage. There is a vast range of potential applications. To realise these requires understanding of the preparation and characterisation of the materials.

This contract is directed specifically to the development and characterisation of optically active materials which have high nonlinear optical activity or laser characteristics. The use is made of the pre-formed sol-gel glass matrix which is doped with optically active material such as organic dye molecules to make nonlinear optically active material for optical limiting and reverse saturable absorption, to make solid state tunable laser systems or to match refractive index of the porous sol-gel glass.

This Annex is concerned with the three main aspects of this programme

- i. Preparation, characterisation and microstructural aspects of optical composites.

This part is important in the development of the material, the fabrication techniques and to give an understanding of the microstructural properties.

- ii. Solid state tunable lasers based on dye doped sol-gel glasses.

Doped sol-gel glasses with organic dyes makes solid state tunable lasers. The properties of the lasers are dependent on the starting materials and fabrication and the use of refractive index matching.

iii. Nonlinear optical characterisation.

The fabrication and properties of nonlinear components for optical limiting and reverse saturable absorption has been investigated using the post-doping technique. This work has shown that advanced materials for nonlinear optical applications can be developed which have characteristics which are suitable for optical limiting and saturable absorption.

## **2. Preparation, Characterisation and Microstructural Aspects of Optical Composites**

### **2.1. Introduction**

A distinctive feature of the sol-gel process is that it enables one to prepare silicate glasses, for instance for optical applications, at far lower temperatures than is possible using conventional melting or vapour deposition methods [1]. However, sol-gel derived optical materials based solely on inorganic systems such as tetramethoxysilane (TMOS)-derived gels can be very porous unless densification has been achieved at higher temperatures of at least 800°C. Consequently, the as-prepared materials can have low mechanical strength and be difficult to polish by conventional means. Moreover, if the pore dimensions of the sol-gel matrix are compatible with the wavelength of incident light then scattering losses may be high.

An attractive way to overcome these problems is to combine properties of very different materials in one, and to produce molecular-scale composite materials via sol-gel processing which have the possibility of improved optical and mechanical properties. A typical example of this is to introduce an organic phase into an essentially inorganic matrix to form an organic-inorganic hybrid materials. Sanchez and Ribot [2] have recently defined two general classes of such hybrid materials, for convenience. Class I corresponds to hybrid systems in which organic molecules, oligomers or low molecular weight organic polymers are simply embedded in the inorganic matrices. In this class, the organic and inorganic components are bonded together via rather weak bonding force mainly through Van der Waals, hydrogen or ionic interactions. Both dye doped (either pre-doped or post-doped) and PMMA-impregnated gel silica glasses fall into this class. Class II corresponds to hybrid organic-inorganic compounds where both organic and inorganic components are bonded through stronger covalent or ionic-covalent bond, hence the organic component is grafted to the inorganic network rather than embedded in it. Where the inorganic network is sol-gel derived silica then the latter have been referred to as ORMOSILs i.e. organically modified silicates [3]. Seddon has expanded Sanchez and Ribot's classification by suggesting that when an active species is doped into an ORMOSIL matrix the as-produced hybrid material should be a Class III type as it represents a combination of their Class I and Class II [4]. Thus, the doped species is embedded into an O-I grafted matrix.

In this section, PMMA-impregnated gel silica glasses (Class I type) and the methyltrimethoxysilane (MTMS)/tetramethoxysilane (TMOS) derived ORMOSIL (Class II type) are characterised in relation to the microstructure of the materials using FT-Raman and near infrared (NIR) spectroscopies. We intended to understand the role of organic components in the formation of the sol-gel structure and their effects on the properties of the finished materials. Laser dye and NLO dye doped ORMOSILs (Class III type) and PMMA/gel silica glass composites are characterised respectively in Section 3 and Section 4 in relation to their lasing and non-linear optical properties.

## **2.2. Experimental**

### **2.2.1. Sample Preparation**

#### **PMMA-Impregnated Gel Silica Glasses**

The monomer, MMA, was freed of inhibitor (hydroquinone monomethyl ether) by washing 3 times with a 5% NaOH-20% NaCl solution followed by repeated washing with distilled water. MMA was then dried overnight with anhydrous sodium sulfate and for a minimum of 48 hours over 4Å molecular sieves. Dried MMA was distilled under reduced pressure at about 35°C prior to use. The TMOS-derived gel silica glasses were initially dehydrated *in vacuo* for 24 hours at room temperature, and impregnated by immersion in a 0.125% benzoyl peroxide/MMA solution overnight in a sealed container. Then, the container was unsealed, transferred to a pressurised reaction vessel under 30 lbs/in<sup>2</sup> N<sub>2</sub> pressure and kept at 60°C for 3 days for polymerisation to proceed. The samples were then detached from the container and polished to obtain smooth surfaces.

#### **MTMS/TMOS Derived ORMOSILs**

MTMS [CH<sub>3</sub>Si(OCH<sub>3</sub>)<sub>3</sub>] and TMOS [Si(OCH<sub>3</sub>)<sub>4</sub>] were combined in 0.5 molar proportions and reacted at room temperature, at low pH, with water. Rods and discs were cast, gelled and dried below 100°C. Sample surfaces were ground and polished in nonaqueous conditions and stored in polythene bags prior to measurements.

## 2.2.2. Characterisation Techniques

### FT-Raman Spectroscopy

Raman experiments were performed using a Perkin-Elmer 1720X FT Raman spectrometer. Raman spectra were excited using the 1064 nm line of a Nd:YAG laser and recorded in the range of 0-3500  $\text{cm}^{-1}$ . A 180° scattering configuration was adopted for data collection. The InGaAs detector of the spectrometer was used at liquid nitrogen temperature to reduce spectral noise. 100 scans were accumulated at a spectral resolution of 4  $\text{cm}^{-1}$ .

### NIR Spectroscopy

Transmission near IR spectra were recorded separately in the 870-1350 nm and 1200-2400 nm region using a Perkin-Elmer Lambda 9 UV-VIS-NIR spectrophotometer operating at a scan speed of 240 nm/min.

For all the Raman and NIR measurements, samples were initially dehydrated *in vacuo* for 72h at ambient temperature and then spectra were recorded under an atmosphere of high purity nitrogen. Subsequent rehydration was performed by letting air into the sample cell under ambient conditions.

## 2.3. Results and Discussion

### 2.3.1. FT-Raman Spectroscopic Study of Methyl-Modified Silica Xerogel

The MTMS/TMOS derived ORMOSIL is characterised in comparison with the TMOS derived silica xerogel. The former contains methyl groups chemically bonded to the Si-O-Si siloxane bond-linked skeleton structure similar to that in the latter. Therefore, it is also called methyl-modified silica xerogel.

The Raman spectrum of the methyl-modified ORMOSIL sample is given in Fig. 2.1. Table 2.1 shows the frequencies and assignment for the bands observed together with those for TMOS-derived gels. In general, the Raman spectrum of the as-prepared sample contains fewer vibrational bands compared with the infrared spectra of the methyl-modified silicates prepared from a similar MTMS/TMOS system upon hydrolysis/polycondensation [5].

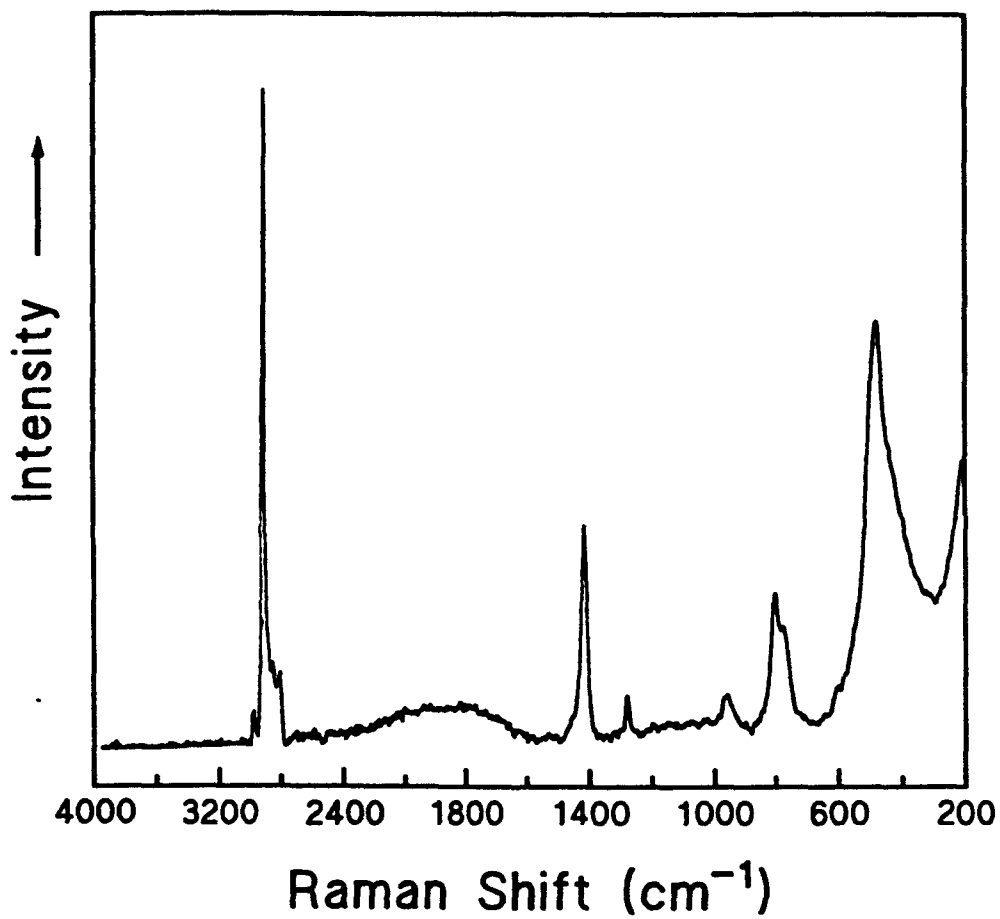


**Fig. 2.1.** FT-Raman spectrum of methyl-modified gel silica derived from MTMS/TMOS system.

**Table 1** Raman spectroscopic data and spectral assignments

MTMS/TMOS derived silica xerogel			TMOS derived silica xerogel [6]		
Frequency $\nu/\text{cm}^{-1}$	Relative intensity	Assignment	Frequency $\nu/\text{cm}^{-1}$	Relative intensity	Assignment
430	sh	$\delta(\text{Si-O-Si})$ , i.p.	430	sh	$\delta(\text{Si-O-Si})$ , i.p.
475	vs	D <sub>1</sub> , trisiloxane ring	485	vs	D <sub>1</sub> , trisiloxane ring
594	w	D <sub>2</sub> , tetrasiloxane ring	600	w	D <sub>2</sub> , tetrasiloxane ring
768	m	$\nu(\text{Si-C})$ of Si-CH <sub>3</sub> $\nu_s(\text{Si-O-Si})$ , TO	795	w	$\nu_s(\text{Si-O-Si})$ , TO
800	m	$\rho(\text{CH}_3)$ of Si-CH <sub>3</sub> $\nu_s(\text{Si-O-Si})$ , LO	815	w	$\nu_s(\text{Si-O-Si})$ , LO
956	w	$\nu(\text{Si-OH})$	975	m	$\nu(\text{Si-OH})$
1275	w	$\delta_s(\text{CH}_3)$ of Si-CH <sub>3</sub>	1060	vw	$\nu_{as}(\text{Si-O-Si})$ , TO
1423	s	$\delta_a(\text{CH}_3)$ of Si-CH <sub>3</sub>	1170	vw	$\nu_{as}(\text{Si-O-Si})$ , LO
2925	vs	$\nu_s(\text{C-H})$ of Si-CH <sub>3</sub>			
2975	vw	$\nu_a(\text{C-H})$ of Si-CH <sub>3</sub>			

Abbreviations: vs = very strong; s = strong; m = medium; w = weak; vw = very weak; sh = shoulder;  
i.p. = in plane

In the  $3000\text{ cm}^{-1}$  region, the band at  $2925\text{ cm}^{-1}$  dominates and it has been assigned here to the symmetrical stretching vibration of C-H bonds of SiCH<sub>3</sub>. The corresponding asymmetrical stretching mode, which possesses the higher relative intensity than the symmetrical mode in the IR spectrum [5], only appears as a very weak peak at  $2975\text{ cm}^{-1}$ . A similar reverse in intensity is observed for the CH<sub>3</sub> deformation bands at  $1423$  and  $1275\text{ cm}^{-1}$ , which have been assigned to the asymmetric and symmetric mode, respectively.

A medium intensity band at *ca.*  $800\text{ cm}^{-1}$  is assigned to the methyl rocking vibration of the SiCH<sub>3</sub> group and the band at  $768\text{ cm}^{-1}$  to the Si-C stretching vibration. However, the latter two assignments are not unique. According to the Raman spectroscopic study on TMOS-derived gel silica by Perry *et al.* [6], there are two bands associated with longitudinal optical (LO) and transverse optical (TO) modes of the Si-O-Si symmetric stretching vibration present in the vicinity of  $800\text{ cm}^{-1}$  at *ca.*  $815$  and  $795\text{ cm}^{-1}$ , respectively. Considering that the Si-O-Si bond still remains as a



skeleton structure in the methyl-modified gel silica, the LO and TO modes should still be expected in this region. According to Perry *et al.*'s study, the LO mode, which appears at a higher wavenumber than the TO mode, should be lower in its intensity than the TO mode and also they tend to be poorly resolved with respect to each other. Furthermore, the overall intensity of the both modes in the TMOS-derived gels is low, in particular for the samples thermally treated at low temperatures. These observations for the inorganic silica xerogel contrast with the spectral features found here for the methyl modified silica. Thus, as shown in Fig. 2.1, the band at  $800\text{ cm}^{-1}$  possesses a higher intensity than that at  $768\text{ cm}^{-1}$ , both are well resolved and the overall intensity of the two is also moderately high.

According to Schmidt and Seiferling [3], an introduction of an organic group into an inorganic network may act in two basically different ways: as a *network modifier* or as a *network former*. Both functions can be realised in ORMOSILs. A suitable way to achieve this is the use of organosubstituted silicic acid esters of the general formula  $R_n'Si(OR)_{4-n}$ , where R' can be any organofunctional grouping. If R' is a non-reactive group, it will have a network modifying effect; if it can react with itself or additional components, it acts as network former. By this definition, a methyl group attached to silicon is a network modifier in the simplest form and it terminates the formation of Si-O-Si siloxane bonds. Therefore, like the TMOS-derived gel silica, Si-O-Si bonds still form the basic backbone structure in the methyl-modified gel silica, where methyl groups are chemically bonded to the skeleton structure. Consequently, the bands related to the Si-O-Si and Si-OH functional groups can be assigned in comparison with the TMOS-derived gel silica [6]. The strong peak at  $475\text{ cm}^{-1}$  and weak peak at  $594\text{ cm}^{-1}$  are Raman active defect  $D_1$  and  $D_2$  bands which have been ascribed to the breathing vibrations of tetrasiloxane and trisiloxane rings in the network structure [7, 8]. Compared with their counterparts in the TMOS-derived gel silica where the  $D_1$  and  $D_2$  bands appear at *ca.*  $485$  and  $600\text{ cm}^{-1}$  respectively, the two bands have red-shifted to lower frequencies. We attribute this to a more open and less strained overall structure in the ORMOSIL material, which allows easier breathing vibrations of the rings. The role of the methyl group as a network modifier is well displayed here by its ability to interrupt a 3D-network structure of Si-O-Si siloxane bonds. An analogy can be made with the alkali ions modified silicate glasses, where alkali ions such as  $Na^+$  interrupt the silica structure by replacing  $Si^{4+}$ . Such a network terminated structure may also explain the appearance of more strained trisiloxane rings in the network structure at temperatures even below  $100^\circ\text{C}$ . It has been reported that the trisiloxane ring related  $D_2$  band did not appear in the Raman spectra of the TMOS-derived gel silica even when the gel was thermally treated at  $180^\circ\text{C}$  [6]. This can be explained by

the schemes shown in Fig. 2.2. According to Brinker *et al.* [7, 8], trisiloxane ring is formed following Scheme 1, i.e. the cyclic ring is formed from the same polymer chain. But it is possible that the trisiloxane ring may be created following Scheme 2, where the cyclic ring is condensed from different polymer chains. Clearly, an increase in polymer chain number and a reduction in chain length will encourage Scheme 2. The presence of a non-reactive, network terminating organic group such as the methyl group might be expected to lead to more polymer chains of shorter length during the sol-gel process compared with the corresponding inorganic system. Therefore, we attribute an early appearance of the trisiloxane ring in the methyl modified gel silica mainly to Scheme 2. Moreover, the more open structure created by the participation of non-reactive organic groups in the network will also better accommodate the more strained trisiloxane rings. From the relative intensities  $D_1$  and  $D_2$  bands it is concluded that the tetrasiloxane rings are predominant in methyl modified silica as is the case for the inorganic silica xerogel.

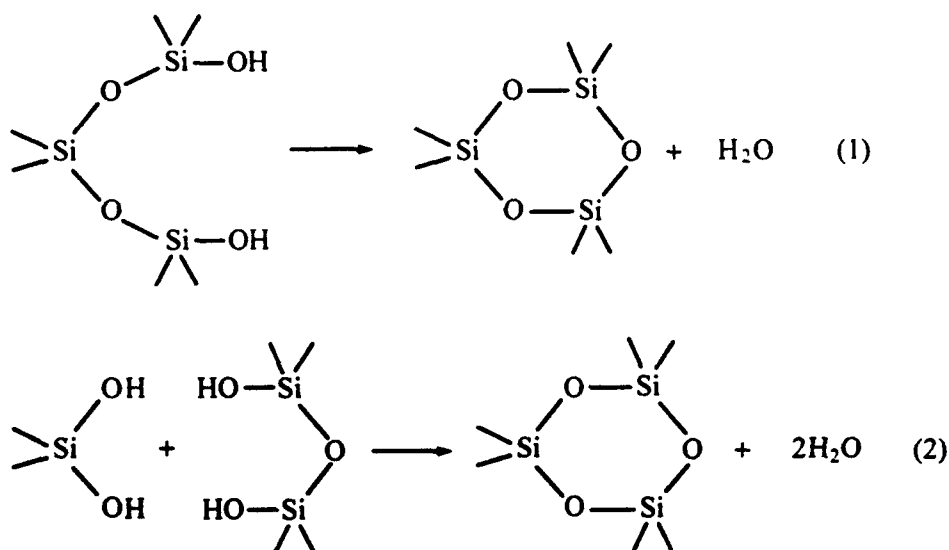


Fig. 2.2. Schemes for the formation of cyclic trisiloxane rings.

The  $D_1$  band is asymmetric and the shoulder on its lower wavenumber side is assigned to in-plane Si-O-Si bending vibration by analogy with the Raman spectra of inorganic silica xerogels [6]. The shoulder is less obvious compared with its counterpart in the

Raman spectrum of the TMOS-derived gel silica, where a well developed broad shoulder at *ca.* 430  $\text{cm}^{-1}$  can be clearly seen [6]. For the inorganic silica xerogel, a concurrent increase in intensity of the Si-O-Si bending band with increasing densification temperature has already been reported [6]. This has been attributed to an increase in Si-O-Si bridging siloxane bonds caused by further polycondensation at higher densification temperatures. When the Si-O-Si siloxane structure is well developed, the Si-O-Si bending band outgrows the  $D_1$  band and becomes completely distinct. For a similar reason, therefore, the lower intensity of the Si-O-Si bending band for the methyl-modified gel silica may be explained by an overall reduction of Si-O-Si linkages in the MTMS/TMOS-derived gel silica due to the presence of linkage-preventing methyl groups.

The band at 956  $\text{cm}^{-1}$  has been assigned to the stretching vibration of Si-OH. The band position and profile is insensitive to dehydration/rehydration treatment, which indicates that the hydrogen-bonding between silanol groups and water molecules has little effect on the vibrational mode of the Si-OH bond. However, this band appears at a lower wavenumber than its counterpart in the silica-only sample, which is located at *ca.* 975  $\text{cm}^{-1}$  [6]. This may also indicate a more open and less strained overall structure. Compared with the TMOS-derived gels prepared at similar thermal treatment temperature, the intensity of the band is rather low, indicating a lower Si-OH concentration in the system. We believe that this is due mainly to the substitution of Si-CH<sub>3</sub> for Si-OH in the system. We also propose that the tendency for more polymer chains of shorter length involved in ORMOSIL preparation will increase mobility and flexibility of the chains and facilitate the polycondensation reactions. Therefore, we also attribute the low Si-OH concentration partly to a more efficient dehydroxylation process.

In the case of the TMOS-derived gel silica, a pair of bands have also been observed at *ca.* 1170 and 1060  $\text{cm}^{-1}$ , which are assigned to the LO and TO modes of the antisymmetric stretching of the Si-O-Si, respectively [6]. However, the corresponding pair in the methyl-modified gel silica are barely visible. But the infrared spectroscopic study on the methyl-modified gel silica did show a strong presence of the two modes [5]. This is a good example of 'complementarity' of IR and Raman spectra. Considering the difference in the vibrational mechanisms between infrared and Raman spectra, an infrared-active vibrational mode may be Raman-inactive, or vice versa, depending upon the symmetry of the vibrational unit. A comparison between IR and Raman spectra of the TMOS-derived gel silica shows that the Si-O-Si antisymmetric stretching mode is Raman-inactive to a large extent [6]. However, the

feature of its LO-TO splitting does show a development with increasing densification temperature. Similarly, this can be explained by an increase in Si-O-Si linkages in the gel network structure. Because the overall Si-O-Si siloxane bonds are reduced considerably in the methyl-modified gel silica, the Si-O-Si antisymmetric band is expected to be very weak.

Our results show that the O-H stretching vibrations associated with water and silanol are absent in the Raman spectrum under the experimental conditions applied. Although both are featured in infrared spectra, a detailed study on these bands is impossible because of the overlapping of these bands in the region above  $3300\text{ cm}^{-1}$ . However, this problem can be easily overcome using NIR spectroscopic method as the combinational bands of the fundamentals associated with different O-H species are well separated, which allows a detailed study on molecular interactions between these different species [9].

### 2.3.2. NIR Spectroscopic Study of PMMA/Gel Silica Glass Composites

The PMMA/gel silica glass composite was characterised comparatively with the silica-only sample used as the substrate and PMMA-only sample. Their NIR spectra, which were recorded separately in the 1200-2500 nm and 870-1350 nm regions, are shown in Figs. 2.3 and 2.4. The related spectroscopic data and spectral assignments are given in Table 2.2

For the silica-only sample, Fig. 2.3a, the 1200-2500 nm region contains three sets of bands with two prominent absorptions occurring at 1370 and 2200 nm. The peak at 1370 nm is sharp and is assigned as the first overtone of the fundamental of O-H stretch of 'free' silanol groups [10]. The peak at 2200 nm is broader and more intense, and is assigned to a combination of the fundamental O-H stretching of 'free' SiOH groups with the fundamental symmetric stretching mode of the silica network at *ca.*  $800\text{ cm}^{-1}$  [10]. The weak band at 1900 nm arises from the combination of stretching and deformation modes of water adsorbed on the gel silica glass. The presence of water may create the hydrogen-bonded silanol species as represented in Fig. 2.5b-d. However, the profile of the spectrum indicates that surface silanol groups exist predominantly as 'free' isolated species as shown in Fig. 2.5a.

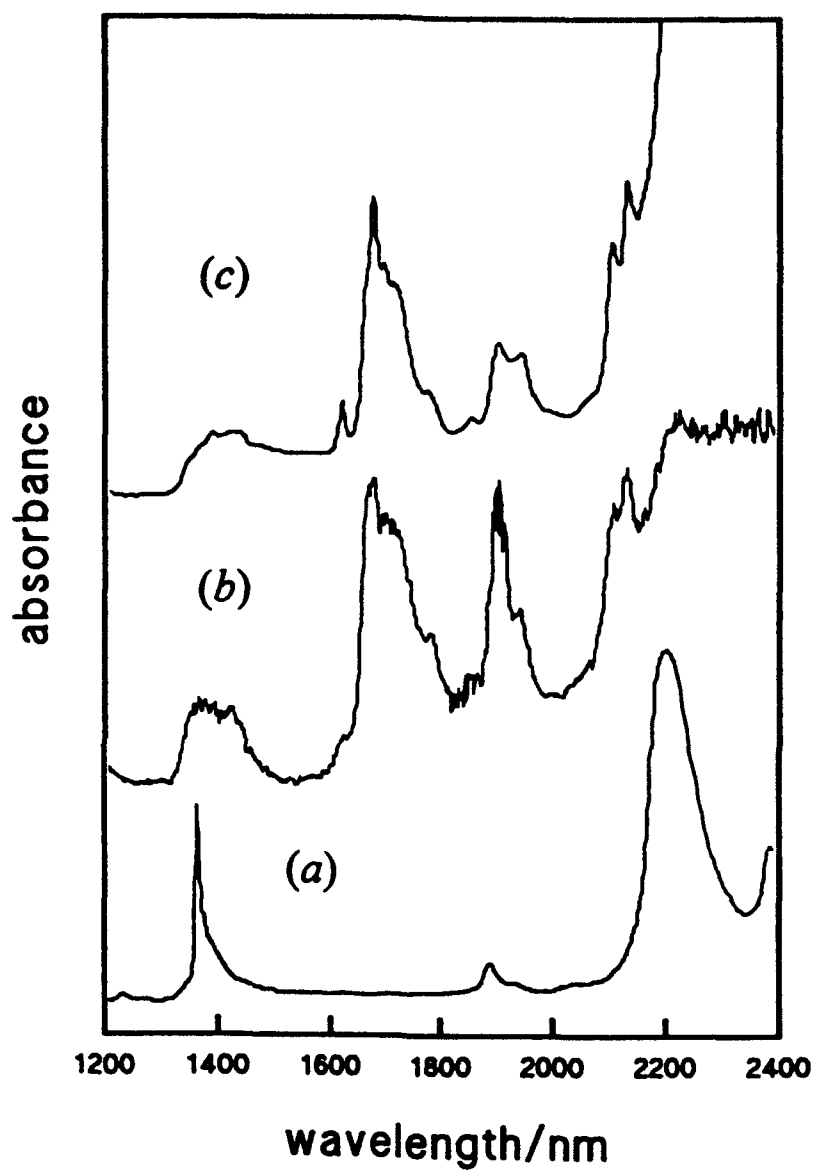


**Fig. 2.3.** NIR spectra in the 1200-2400 nm region. (a) gel silica glass. (b) PMMA. (c) PMMA/gel silica glass composite.

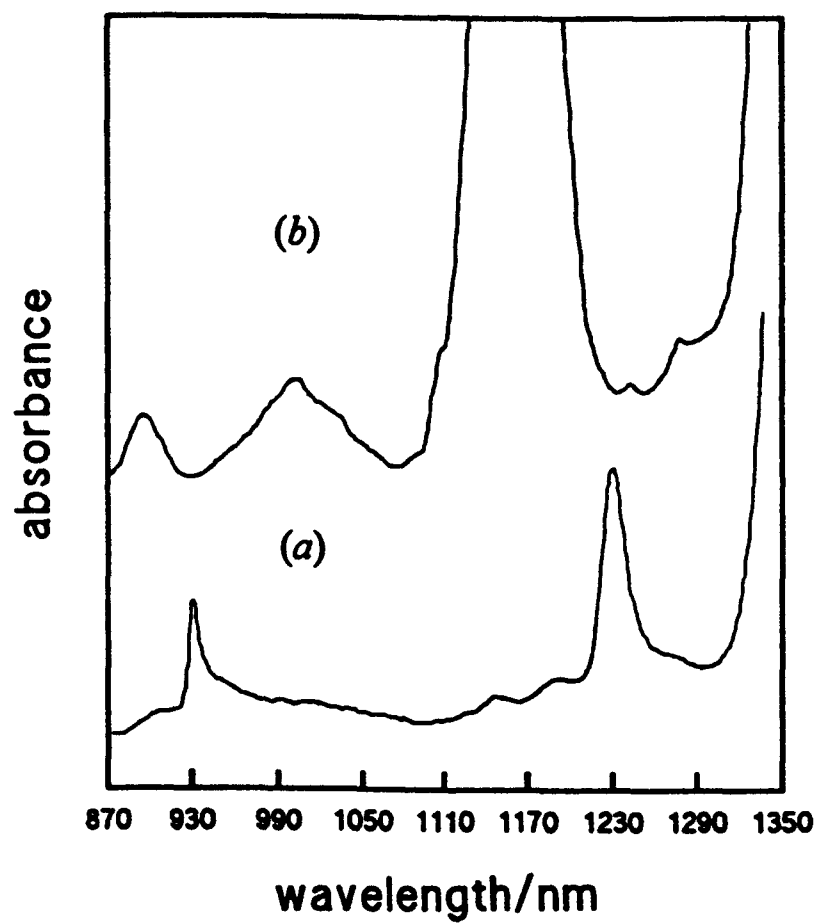


**Fig. 2.4.** NIR spectra in the 870-1350 nm region. (a) gel silica glass. (b) PMMA/gel silica glass composite.

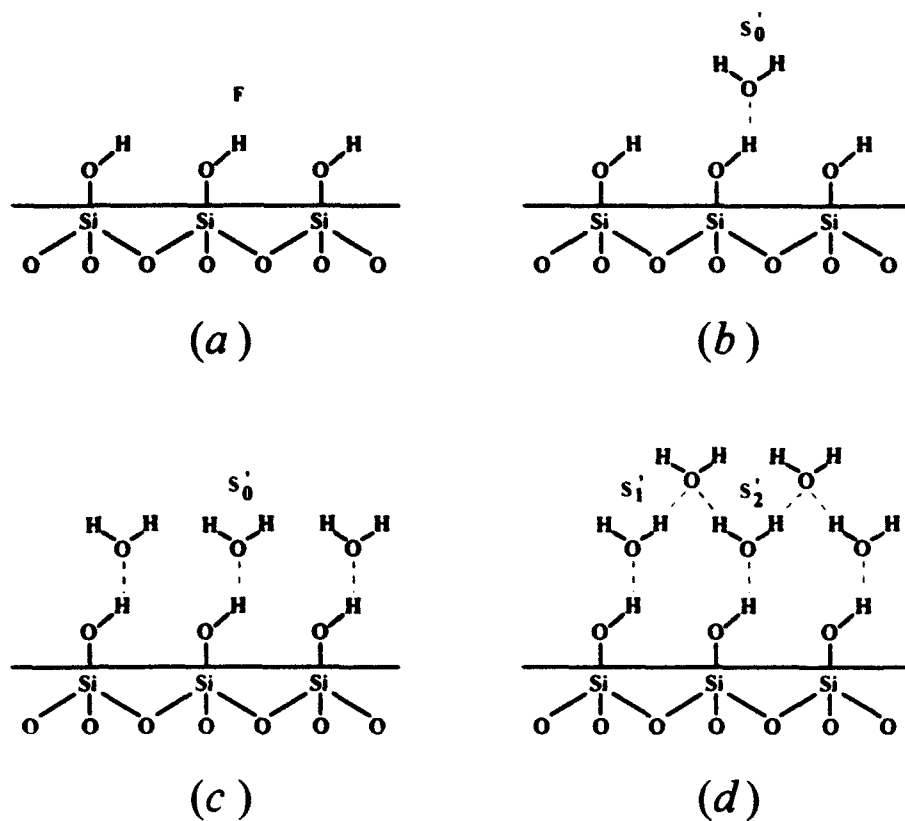


**Fig. 2.5.** Pictorial representation of surface silanol species and adsorbed water species. F: free or non H-bonded silanol.  $S_0'$ : monomerically adsorbed water.  $S_1'$ : partially H-bonded water.  $S_2'$ : fully H-bonded water.

**Table 2** NIR spectroscopic data and spectral assignments

gel SiO <sub>2</sub> glass			PMMA/gel SiO <sub>2</sub> glass composite		
$\nu/\text{cm}^{-1}$	$\lambda/\text{nm}$	assignment	$\nu/\text{cm}^{-1}$	$\lambda/\text{nm}$	assignment
4562	2192	$\nu_{\text{OH}}(\text{SiOH}; \text{F}) + \nu_{\text{s}}(\text{Si-O-Si})$	1451	6892	$\delta_{\text{CH}}(-\text{CH}_2, >\text{CH}_2)$
5155	1940	$\nu_{\text{OH}} + \delta_{\text{HOH}} (\text{H}_2\text{O}; \text{S}_1', \text{S}_2')$	1639	6101	$\nu_{\text{C=C}}(\text{MMA})$
5263	1900	$\nu_{\text{OH}} + \delta_{\text{HOH}} (\text{H}_2\text{O}; \text{S}_0')$	1699 sh	5886	$\nu_{\text{C=O}}(\text{H-bonded to SiOH})$
7331	1364	$2\nu_{\text{OH}}(\text{SiOH}; \text{F})$	1723	5804	$\nu_{\text{C=O}}(\text{not H-bonded})$
8123	1231	$2\nu_{\text{OH}}(\text{SiOH}; \text{F}) + \nu_{\text{s}}(\text{Si-O-Si})$	1727	5794	$\nu_{\text{C=O}}(\text{PMMA})$
8418	1188	$2\nu_{\text{OH}} + \delta_{\text{HOH}} (\text{H}_2\text{O}; \text{S}_1', \text{S}_2')$	4348	2300 b	$\nu_{\text{CH}} + \delta_{\text{CH}} (-\text{CH}_2, >\text{CH}_2)$
8757	1142	$2\nu_{\text{OH}} + \delta_{\text{HOH}} (\text{H}_2\text{O}; \text{S}_0')$			$\nu_{\text{OH}}(\text{SiOH}; \text{H}) + \nu_{\text{s}}(\text{Si-O-Si})$
10753	930	$3\nu_{\text{OH}}(\text{SiOH}; \text{F})$	4688	2133	$\nu_{\text{CH}}(-\text{OCH}_3) + \nu_{\text{C=O}}$
			4748	2106	
			5147	1943	$\nu_{\text{OH}} + \delta_{\text{HOH}} (\text{H}_2\text{O}; \text{S}_1', \text{S}_2')$
			5255	1903	$\nu_{\text{OH}} + \delta_{\text{HOH}} (\text{H}_2\text{O}; \text{S}_0')$
			5394	1854	$4\nu_{\text{CO}}(\text{O-CH}_3)$
			5627	1777	$2\nu_{\text{CH}}(>\text{CH}_2)$
			5831	1715	
			5900	1695	$2\nu_{\text{CH}}(-\text{CH}_3)$
			5963	1677	
			6180	1618	$2\nu_{\text{CH}}(=\text{CH}_2; \text{MMA})$
			7143	1400 b	$2\nu_{\text{CH}} + \delta_{\text{CH}} (-\text{CH}_2, >\text{CH}_2)$
					$2\nu_{\text{OH}}(\text{SiOH}; \text{H})$
					$2\nu_{\text{OH}}(\text{H}_2\text{O}; \text{S}_0')$
					$2\nu_{\text{OH}}(\text{H}_2\text{O}; \text{S}_1', \text{S}_2')$
			7813	1280	$2\nu_{\text{CH}}(-\text{CH}_3) + \nu_{\text{C=O}}$
			8032	1245	$2\nu_{\text{OH}}(\text{SiOH}; \text{H}) + \nu_{\text{s}}(\text{Si-O-Si})$
			8540	1171 b	$3\nu_{\text{CH}}(-\text{CH}_3)$
					$3\nu_{\text{CH}}(>\text{CH}_2)$
					$2\nu_{\text{OH}} + \delta_{\text{HOH}} (\text{H}_2\text{O}; \text{S}_0')$
					$2\nu_{\text{OH}} + \delta_{\text{HOH}} (\text{H}_2\text{O}; \text{S}_1', \text{S}_2')$
			9009	1110 sh	$3\nu_{\text{CH}}(=\text{CH}_2)$
			9990	1001 b	$3\nu_{\text{CH}} + \delta_{\text{CH}} (-\text{CH}_3, >\text{CH}_2)$
			11173	895	$4\nu_{\text{CH}}(-\text{CH}_3)$
					$4\nu_{\text{CH}}(>\text{CH}_2)$

Abbreviations: F = free; H = hydrogen-bonded; S<sub>0</sub>' = monomeric; S<sub>1</sub>' = partially hydrogen-bonded; S<sub>2</sub>' = fully hydrogen-bonded; sh = shoulder; b = broad.



In the 870-1350 nm region, Fig. 2.4, there are also three principal groups of absorption bands for the silica-only sample, but with much reduced intensities. The band at 1231 nm is assigned to a combination of the first overtone of the O-H stretch for 'free' silanol groups with the Si-O-Si symmetric stretch of the silica network [10]. The band at 930 nm is assigned as the second overtone of the fundamental stretch of the 'free' SiO-H groups. Weak peaks at 1145 and 1190 nm correspond, respectively, to adsorbed monomeric water with its oxygen hydrogen-bonded to SiOH groups ( $S_0$  species), Figure 2.5b and 2.5c, and water molecules hydrogen-bonded to SiOH groups as well as with one another ( $S_1$  and  $S_2$  species), Fig. 2.5d.

For the PMMA/silica composite materials, the absorption profiles in both of the spectral regions differ distinctively from that of the silica-only sample. In general, there are several broad absorption bands in the regions around *ca.* 870, 1000, 1170, 1400, 1700 and 2300 nm, which cover almost the whole the near infrared. A comparison shows that these additional features are largely attributed to the PMMA present in the gel silica matrix.

#### 2.3.2.1. Spectral Analysis in the 1200-2500 nm Region

As far as vibrational spectroscopy is concerned, the absorption bands in the near IR are due to overtones and combinations of the fundamental mid-IR vibrational bands. The most prominent bands are those related C-H, N-H, and O-H groups. The very strong band at *ca.* 2300 nm should be attributed at least partly to the combinations of C-H stretching and deformation fundamentals of methyl ( $\alpha$ -CH<sub>3</sub> and CH<sub>3</sub>-O) and methylene (CH<sub>2</sub>) groups from PMMA, which is in agreement with the general assignments for the similar kind of functional group in organic compounds [11]. However, a comparison shows that the 2300 nm band is more intense for the composite than for PMMA. Obviously, the increase in intensity should be attributed to a contribution from the combinational vibrations of the fundamental stretchings of the SiO-H and the silica skeleton which have been shown to be present in the region.

There are a number of bands grouping in the 1700 nm region. According to the general understanding [11], the fundamental carbon-hydrogen stretching vibrations of methyl (CH<sub>3</sub>) groups appear at slightly shorter wavelengths than those of methylene (CH<sub>2</sub>) groups and their first overtones occur in the 1700 nm region in the form of a doublet. Therefore, we have assigned the doublet at 1677 and 1695 nm to methyl groups and one at 1715 and 1777 nm to the methylene group. According to Wheeler

[11], a very weak band at 1854 nm has been assigned to the third overtone of the single-bond fundamental carbon-oxygen stretching of O-CH<sub>3</sub>.

The band at 1618 nm is sharp and well defined. We have assigned it to the first overtone of fundamental C-H stretching of terminal =CH<sub>2</sub> of MMA, which has not been converted to PMMA during the polymerisation process. Clearly, both NIR and Raman spectral results are compatible with each other, both of which show the presence of MMA in the PMMA/gel silica glass composite (N.B. For the FT-Raman spectra of the PMMA/gel silica glass composites, please see our fourth interim report). Interestingly, under the same preparation conditions, the residual MMA left in the PMMA-only sample is much less. This implies that the conversion of MMA to PMMA is less efficient in the presence of the porous sol-gel matrix. Understandably, very limited space in narrow pore channels limits the mobility of monomer and makes the addition of monomer to the already formed polymer chain less efficient. This is especially true at the later stages of the polymerisation when the viscosity of the medium becomes increasingly large. It is worth noting that increasing initiator concentration is not a good solution to the problem. Although this is able to initiate more reaction sites for monomer addition, it also increases the reaction rates. As a result, the polymerisation could be too quick to have all pore channels fully filled with the polymer. We note that appreciable volume contraction occurs on conversion of MMA to PMMA, of approximately 20%. In other words, fully MMA filled pores prior to polymerisation will only be partially filled with PMMA afterwards unless a continuous supply of MMA is available during the polymerisation. As a result of the partial pore filling, the index matching in these partially filled pores can be so poor that the as-prepared sample scatters light even more seriously than the unfilled sample. Therefore, careful control over the rate of MMA-to-PMMA conversion is indispensable. Ideally, pores should only be closed by the time no empty pore space is left in the matrix.

The presence of residual MMA should also produce a doublet in the 2100 nm region, where the combinational vibrations of the C-H stretch of terminal =CH<sub>2</sub> and C=C stretch are usually observed for alkene [12]. The presence of the bands at 2106 and 2133 nm in Fig. 2.3c is an indication for such vibrational modes. However, the two bands cannot be attributed to =CH<sub>2</sub> and C=C functional groups alone since the two are still well present in the spectrum of PMMA-only sample (Fig. 2.3b), where a higher conversion efficiency of MMA-to-PMMA has been observed, with no major change of their positions and intensities, except that the former becomes less obvious due probably to a reduction of residual MMA concentration. Because there is no

literature-based assignment available, we have assigned the two bands to the combinational vibrations of C-H stretching of  $\text{OCH}_3$  and C=O stretching of ester carbonyl.

The methyl and methylene groups in PMMA are also partly responsible for the broad band in the 1400 nm region where the second combinational vibrations of the first C-H stretching overtone and fundamental deformation are located. According to the spectrum of the silica-only sample, the first overtone of the SiOH group also occurs in this region. However, the sharp 'free' silanol band appearing in the spectrum of the silica-only sample is completely missing in that of the PMMA/gel silica glass composite. As we know, the dehydrated silica which leaves its surface silanol groups free from hydrogen-bonding has a strong tendency to readsorb water. As a result, the sharp peak at *ca.* 1365 nm will be broadened at the expense of losing its intensity [9]. The appearance of two bands in the 1900 nm region, which are due to the combinational vibrations of O-H stretching and deformation fundamentals of water, does indicate the possible hydrogen-bonding between SiOH and water. However, according to Perry and Li's study [9] and ours, such quantities of water cannot account for the entire disappearance of the 'free' silanol band. In other words, there must be some other mechanism jointly responsible for the conversion of 'free' silanol to associated species. Viewing the composite system, we notice that the only functional group capable of participating in hydrogen-bonding is the carbonyl group in PMMA. It is deduced that the additional interaction is from the hydrogen-bonding formation between silanol and ester carbonyl group as schematically shown in Fig. 2.6. This argument is strongly backed by our FT-Raman results. As we have already shown above, the carbonyl Raman band of the composite at  $1723\text{ cm}^{-1}$  bears a shoulder at  $1639\text{ cm}^{-1}$  and also slightly shifted to lower wavenumber compared with its symmetrically shaped counterpart at  $1727\text{ cm}^{-1}$  for PMMA. Certainly, this additional feature is closely related to the hydrogen-bonding between silanol and carbonyl.

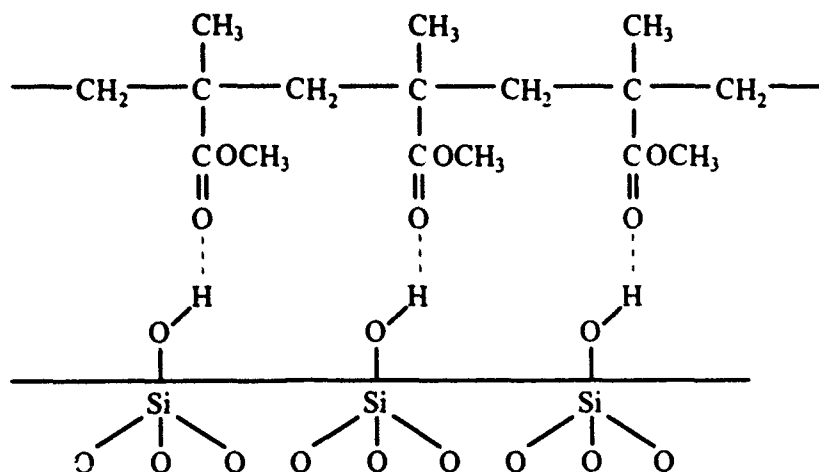


Fig. 2.6. Hydrogen bonding between silanol and carbonyl groups.

However, the model illustrated in Fig. 2.6 is just an idealised case. Viewing the residual water present in the composite system and hydrophilic nature of the partially densified sol-gel glasses, water should also be able to compete with carbonyls from polymer chains for occupying the surface silanol sites. Therefore, the participation of water molecules in hydrogen-bonding with surface silanol groups is expected. According to our Raman spectroscopic results, not all the carbonyl groups are hydrogen-bonded to silanol groups, as indicated by the band at  $1723\text{ cm}^{-1}$  which has already been assigned to carbonyl species free from hydrogen-bonding. Consequently, the majority of carbonyl groups remain unbonded. This is due mainly to insufficient silanol groups being available for hydrogen-bonding and also partly to the occupation of some silanol sites by water molecules. In agreement with Perry and Li's study [9], the silanol groups on the surface of silica are primary adsorbing sites for the formation of the first water layer on the silica surface, which is responsible for the initial formation of  $S_0'$  species; then the  $S_0'$  species can function as the secondary sites for the formation of multi-water layers which subsequently creates the  $S_1'$  and  $S_2'$  species. For the PMMA/gel silica glass composite, therefore, the band at *ca.*  $1900\text{ nm}$  is attributed to monomeric water species ( $S_0'$ ) and the band next to it on the high wavelength side to associated species ( $S_1'$  and  $S_2'$ ). Supposing that water molecules are evenly distributed in the PMMA phase rather than favourably adsorbed on the

silica surface, we would expect that the profile of water bands of the composite should be very similar to that of the PMMA-only sample. However, a comparison shows that water exists predominantly as  $S_0'$  species in the latter, as indicated by its related band at *ca.* 1900 nm in Fig. 2.3b, and the intensity of its counterpart in the former is much reduced with a relative increase in proportion of  $S_1'$  and  $S_2'$  species (Fig. 2.3c). This indicates that such an increase in associated water species in the composite is directly related to the local enrichment of water on the silica surface as a result of the initial bonding between water and silanol and the secondary bonding between water molecules themselves.

Notably, the relative proportion of  $S_1'$  and  $S_2'$  species is even higher in the composite than in the silica-only sample when similar amounts of adsorbed water on the surface are considered. It has been shown [9] that for the silica-only sample,  $S_0'$  species are predominant at low water concentration and the resolved  $S_1'$ ,  $S_2'$  band only develops at the later stage of hydration. However, for the PMMA/gel silica glass composite, the band associated with  $S_1'$  and  $S_2'$  species is completely resolved from the  $S_0'$  band even at the low concentration of residual water. This can be explained by the formation of hydrogen-bonding between silanol and carbonyl, which makes some silanol sites no longer available for water molecules. Therefore, some water molecules which could be initially hydrogen-bonded to SiOH groups tend to associate themselves with those water molecules which have already existed as  $S_0'$  species. Consequently, the importance of water molecules as secondary adsorbing sites within the composite is increased. According to the Perry and Li's model, this is directly responsible for the formation of  $S_1'$  and  $S_2'$  species.

#### 2.3.2.2. Spectral Analysis in the 870-1350 nm Region

The 870-1350 nm region contains higher overtones and combinations of the fundamental vibrations. Compared with those in the 1200-2400 nm region, all bands in the region are significantly weaker and also exhibit narrowed separation of bands owing to anharmonic features for the vibrations involved.

The strongest band at 1171 nm in the region is assigned to the second overtones of fundamental C-H stretchings from  $-CH_3$  and  $>CH_2$ , with no further distinguishing between the two. According to the spectrum for the silica-only sample, the second combinational bands of water should appear at *ca.* 1140 and 1190 nm which correspond to  $S_0'$ , and  $S_1'$ ,  $S_2'$  species, respectively. Compared with the first combinational bands of water in the 1900 nm region, where they are well separated

from the first overtones of C-H stretchings, the water bands are now superimposed with the 1171 nm band. In other words, the C-H bands have red-shifted relative to the water bands. This is attributed directly to the anharmonic nature of molecular vibrations which allows transitions between more than one energy level to happen but lower than exactly two or three times the frequency of the fundamental as observed here for the overtones of fundamental C-H stretching [13, 14]. Because the water bands in the region originate basically from the combination of three fundamental modes which does not involve the overtone bands, their positions are less affected.

The shoulder at 1110 nm is attributed to the second overtone of fundamental C-H stretching of  $=CH_2$  from MMA. The second combinational vibration associated with the unsaturated centre has been assigned to the band at *ca.* 1280 nm. The broad band at 1001 nm can be easily assigned to the third combination of  $-CH_3$  and  $>CH_2$  which also show their third C-H stretching overtone at 895 nm.

As in the 1200-2400 nm region, the higher overtone and combination of SiOH group could not be identified unambiguously in the presence of much stronger bands from PMMA. No free silanol bands at 930 nm and 1231 nm were observed as they are shown in the silica-only sample. However, a weak band at 1245 nm may well be related to the silanol groups, which are mainly hydrogen-bonded to carbonyls groups of PMMA, and therefore whose vibrational absorption energy is red-shifted in relation to the band of 'free' silanol groups at 1231 nm. Accordingly, we assign the 1245 nm band to the second combination of the first O-H stretching overtone of the hydrogen-bonded SiOH groups and the symmetrical Si-O-Si stretching of the silica skeleton.

## 2.4. Conclusions

As a non-reactive group, the methyl group has a chain-terminating effect for stopping the formation of Si-O-Si siloxane bonds. Therefore, it acts as a network modifier rather than a network former in the sol-gel derived ORMOSIL materials. Consequently, the incorporation of methyl groups in the network creates more open structures in the hybrid organic/inorganic MTMS/TMOS derived materials than that in the inorganic, TMOS-derived xerogels. We believe that mobility and flexibility of polymer chains formed in the sol-gel process are increased for the former which leads to a higher efficiency of polycondensation reaction via dehydroxylation of Si-OH groups, and also to an early appearance of more strained trisiloxane rings at lower temperatures than expected for the non-modified system. Formation of the trisiloxane

rings is also favoured by the more open structure. However, the overall bridging Si-O-Si siloxane units are fewer than those in the corresponding inorganic system as expected, due to the substitution of non-condensable Si-CH<sub>3</sub> groups for Si-OH groups.

The impregnated organic PMMA phase interacts with the inorganic silica phase via the hydrogen-bonding between carbonyl and silanol groups. Unlike the ormosil type materials in which organics are chemically incorporated in the network structure, the molecular interaction in the composite prepared by the post-doping method occurs mainly at the boundary of the two phases. Therefore, the bulk chemical properties of each phase should be largely retained. Residual water inherited from the preparation process is not evenly distributed in the composite but locally enriched on the silica surface by hydrogen-bonding to limited silanol adsorbing sites. The conversion efficiency of MMA-to-PMMA depends not only on the polymerisation conditions applied, but also on the initial textual structure of the gel silica glass used. In general, the substrate with more open pore structure and larger pore sizes will facilitate the polymerisation process. It should be mentioned that although organically modified sol-gel glasses show high optical transmittance in the near UV and visible region due to a reduction of scattering from an initially porous structure, their application in the near IR is restricted to some extent due to the combined vibrational energy absorptions by different silanols and water species, in particular by C-H functional groups from organic modifiers.

## 2.5. References

- [1] L.L. Hench and J.K. West, *Chem. Rev.* 90 (1990) 33.
- [2] C. Sanchez and F. Ribot, in: *Proceedings of 1st European Workshop on Hybrid Organic-Inorganic Materials (Synthesis, Properties and Applications)*, Chateau de Bierville, France, Nov. 8-10, 1993, ed. C. Sanchez and F. Ribot.
- [3] H. Schmidt and B. Seiferling, *Mater. Res. Soc. Symp. Proc.* 73 (1986) 739.
- [4] Through personal communication with Dr. A.B. Seddon.
- [5] C.A. Capozzi, R.A. Condrate, Sr. and L.D. Pye, *Mater. Lett.* 14 (1993) 300.
- [6] C.C. Perry, X. Li and D.N. Waters, *Spectrochim. Acta* 47 (1991) 1487.
- [7] C.J. Brinker, D.R. Tallant, E.P. Roth and C.S. Ashley, in: *Defects in Glasses*, ed. F.L. Galeener, D.L. Griscom and M.J. Weber (Materials Research Society, Pittsburgh, 1986) p. 387.

- [8] C.J. Brinker, R.J. Kirkpatrick, D.R. Tallant, B.C. Bunker and B.Montez, *J. Non-Cryst. Solids* 99 (1988) 418.
- [9] C.C. Perry and X. Li, *J. Chem. Soc. Faraday Trans.* 87 (1991) 3857.
- [10] C.C. Perry and X. Li, *J. Chem. Soc., Faraday Trans.* 87 (1991) 761.
- [11] O. H. Wheeler, *Chem. Revs.* 59 (1959) 629.
- [12] I. Murray, in: *Analytical Applications of Spectroscopy*, ed. C.S. Creaser and A.M.C. Davies (The Royal Society of Chemistry, 1988) p. 39.
- [13] K.B. Whetsel, *Appl. Spectrosc. Rev.* 2 (1968) 1.
- [14] L.G. Weyer, *Appl. Spectrosc. Rev.* 21 (1985) 1.



### **3. Solid state tunable lasers based on dye doped sol-gel glasses.**

**M.D.Rahn**

#### **3.1. Experimental program**

The aim of this part of the project is to develop the technology and science of dye doped sol-gel glasses for laser applications. It is hoped that eventually efficient, stable and tunable pulsed high energy lasers based sol-gel glass composites doped with laser dyes will be possible. The main areas of work in this project are to make improvements in laser efficiency and photostability, and they fall into four main areas:-

- Choice of dye and optimising dye's chemical environment
- Optimisation of the host
- Optimisation of the pump source
- Designing a cavity which makes maximum use of each dye molecule before degradation occurs and has maximum efficiency.

The first three items have been addressed using a compact "investigation" cavity which is described below, and the results are used in the design of the optimised cavity in ●, which is yet to be built.

Three dyes for impregnation into sol-gel glass were chosen on the basis of reported efficiency and stability. The perylene dye, KF241, is reported to be highly stable (2,3), the dye pyrromethene 567 is reported to be highly efficient (4,5), and rhodamine 590 is a common well understood efficient dye.

These dyes have been post-doped into densified sol-gel glass blocks which were then index-matched with polymethylmethacrylate (PMMA) by in-situ polymerisation of methylmethacrylate (MMA). The index matched

samples were then optically polished. The finished samples were then tested in the "investigation" cavity for efficiency and photostability using pump sources of varying pulse length and wavelength.

### **3.2. Experimental arrangements.**

All the laser results were taken with an identical cavity. The cavity was of an open type and has no tuning element and the samples were longitudinally pumped through a dichroic input mirror. The output mirror was a broadband 70% reflector. The pump beam was focused down to a spot 2mm in diameter, which means that because the blocks were about 5mm thick that the cavity volume was about  $20\text{mm}^3$ . The pump energy was measured before the focusing lens and the output energy was measured after the output beam had passed through a filter to eliminate any pump light. Both short and long pulse excitation has been investigated. The pump source was either a Quantel Nd:YAG laser operating at the second harmonic, 532nm, with a pulse length of 15ns and a peak pulse energy of 57mJ, or a flashlamp pumped coumarin 504 dye laser emitting 3 $\mu$ s pulses at 504nm.

### **3.3. System lifetime**

Since the system lifetime is one of the most important properties of any sol-gel dye laser, it is important that we have some way of characterising it and describing it in a way that enables a comparison of different systems. If the total accumulated pump energy incident on the system before the system output decreases by half is measured, the resulting figure is a measure of the system lifetime. Since bigger systems can obviously operate for more shots for a given pump pulse energy than small systems, the accumulated pump energy must be divided by the gain

region volume to give a measure of system lifetime which can compare different systems. It is therefore logical to define the system lifetime as "the accumulated pump energy on the system per unit volume of gain region used before the output energy drops by half" and give it units of  $\text{Jmm}^{-3}$ . It may well be more logical to use the definition "the accumulated pump energy on the system per mole of dye molecules in the gain region before the output drops by half" and give it units of  $\text{Jmole}^{-1}$ , but for now the former definition will be used as work published by other authors (6-9) usually only give enough information to calculate the system lifetime as defined by the former definition.

### 3.4. Short pulse excitation results.

#### Rhodamine 590

Table 1 shows an overview of all the main short pulse length excitation results taken to date. A  $3 \times 10^{-4}\text{M}$  solution of Rhodamine 590 in solution was pumped with the Quantel Nd:YAG laser. It showed a good efficiency when pumped in the cavity. Its slope efficiency was 43% and its peak output power was 17.3mJ, which represents an efficiency of 27% and demonstrates saturation due to high pump intensity. Long pulse length results using the flashlamp pumped dye laser as a pump source gave a 13% slope efficiency with a  $3\mu\text{s}$  laser output pulse duration. A  $3 \times 10^{-4}\text{M}$  solution of rhodamine 590 impregnated into a polished PMMA index-matched sol-gel block yielded a 26% slope efficiency and had a peak output power of 13mJ (23%), which shows a reduced degree of saturation. It is not clear why we should observe reduced saturation of rhodamine 590 in sol-gel/PMMA.

The output power as a function of the number of shots was also determined, and the system lifetime measured. With 12.8mJ pump pulses the half-life was 1030 shots out of a gain region of  $20\text{mm}^3$ . This equates to system lifetime of  $0.67\text{Jmm}^{-3}$ , which is the best value reported to date. The

best previously published work was  $0.5\text{Jmm}^{-3}$  obtained by Dunn et al. at U.C.L.A.(6) The system lifetime was measured at several different pump pulse energies and it was found that with higher pulse energies the system lifetime gradually reduced. With pump pulses of  $57\text{mJ}$  the system lifetime reduced to  $0.25\text{Jmm}^{-3}$  (90 shots), as shown in fig 1. It is therefore apparent that to get the most shots out of each dye molecule the pump intensity must be kept to a minimum.

It is also interesting to note that as photodegradation of rhodamine 590 in sol-gel/PMMA occurred, the peak output wavelength shifted from  $572\text{nm}$  to  $563\text{nm}$ . This is probably due to decomposition products absorbing any output light at  $572\text{nm}$  more than any light at  $563\text{nm}$  hence shifting the laser's gain peak.

### **Pyrromethene 567**

Pyrromethene 567 is soluble in ethanol and hence is easy to impregnate into sol-gel via the post doping method. It is reported to be an exceptionally efficient dye. A  $1 \times 10^{-4}\text{M}$  solution of pyrromethene 567 in solution also gave a good efficiency in solution when pumped in the same cavity. Its slope efficiency was also 43%, which compares to 14% when pumped with the flashlamp pumped dye laser. Its peak output was  $24\text{mJ}$ , which corresponds to an efficiency of 42%. No saturation is occurring. Due to the relatively low absorbance of the cuvette of dye (about 0.5 at  $532\text{nm}$  (fig 2)) it was suspected that some pump light may have gone straight through the cavity thus distorting the output energy measurements. When this effect was corrected for, no appreciable change in peak output energy was observed. In fact the percentage of laser output energy as a fraction of total energy falling on the energy meter increased with pump energy. This confirms the theory that no saturation is occurring at high pulse energies and at low pulse energies the offset due to a threshold is appreciable. The slope efficiency in unindex-matched unpolished sol-gel was measured to be 20%, but the peak output energy was not measured due to the possibility of laser damage. The system lifetime was measured

to be  $0.13\text{Jmm}^{-3}$  with a  $8.1\text{mJ}$  pump pulse energy. The system lifetime decreases with pump pulse energy (intensity) here too. This lower value for system lifetime can be attributed to air filled pores which contain oxygen. PMMA impregnation is hoped to improve this value. Unlike the rhodamine 590 system the peak output wavelength did not shift, indicating the possibility that the decomposition products are transparent.

### Short pulse length laser optimisation.

Fig 3, shows a possible optimised laser configuration. It is yet to be designed in detail but the size of the block could be  $5 \times 5 \times 20\text{mm}$  and the concentration of dye in this size block would be about  $1 \times 10^{-4}\text{M}$ . This contains  $5 \times 10^{-8}$  Moles of dye. The previous exploratory laser system had a  $20\text{mm}^3$  gain volume with a concentration of  $3 \times 10^{-4}\text{M}$ . this contained  $6 \times 10^{-9}$  Moles of dye. If we now assume that the photostability of dye molecules is independent of concentration, we can use the results presented in this report to make a forecast of the performance of this optimised laser system.

For this forecast we use the measured value of system lifetime,  $L$ , as measured in  $\text{JMole}^{-1}$  and also calculate the pump intensity,  $I$ , in units of  $\text{mJpulse}^{-1}\text{Mole}^{-1}$  of dye molecules contributing to laser action during the lifetime of the system.

The pump pulse energy,  $P_N$ , of the new system which corresponds to an equal pump intensity to that of the original system is given by:-

$$P_N = IM_N = \frac{P_O}{M_O} M_N \quad (1)$$

where  $M$  is the number of moles of dye and the subscripts  $O$  and  $N$  refer to original and new systems respectively.

The output energy  $E_N$  of the new system is given by the pump pulse energy of the new system multiplied by the efficiency of the original system,  $\epsilon$ .

$$E_N = \epsilon P_N = \epsilon P_O \frac{M_N}{M_O} \quad (2)$$

The half life of the new system in number of pulses ( $N$ ) can be calculated using the system lifetime of the original system measured at  $P_O$  ( $L$ ), and is given by:-

$$\text{Pulses} = N = \frac{LM_N}{P_N} \quad (3)$$

If we consider low energy operation of the new system, using rhodamine 590 in index-matched polished sol-gel/PMMA and corresponding to  $P_O=8\text{mJ}$ , the above equations give us:-

- $P_N=65\text{mJ}$
- $E_N=36\text{mJ}$  ( $\epsilon=43\%$ )
- $\text{Pulses}=1500$ .

If we consider high energy operation of the new system, corresponding to  $P_O=60\text{mJ}$ , the above equations give us:-

- $P_N=500\text{mJ}$
- $E_N=180\text{mJ}$  ( $\epsilon=27\%$ )
- $Pulses=55$ .

These figures assume that the efficiency of these dyes in sol-gel/PMMA will eventually almost match the efficiency in solution. It must also be noted that in the future improvements in  $L$  (lifetime) are expected to be made.

### 3.5. Long pulse length excitation results.

#### Rhodamine 590.

Rhodamine 590 in sol-gel has been investigated with a flashlamp pumped coumarin 504 dye laser used as a pump source. Table 2 shows the results for rhodamine 590 and shows a 13% slope efficiency.

The most striking result is the factor of about a thousand increase in threshold from the nanosecond pump pulses to the microsecond pump pulses for rhodamine 590 in sol-gel and the subsequent decrease by almost a factor of three after PMMA impregnation and polishing of the sol-gel surfaces.

The photostability results for rhodamine 590 in sol-gel when pumped with the flashlamp pumped dye laser are also given in table 2. The full power lifetime was  $0.03\text{Jmm}^{-3}$ . After impregnation with PMMA, the number of shots increased significantly. When pumped with  $110\text{mJ}$  pulses with a rep rate of one shot per minute initially 15 shots of laser action were observed. After leaving the sample for several hours to recover, 5 more shots were observed showing dye recombination in sol-gel/PMMA. Eventually a total of 35 shots was emitted by a  $20\text{mm}^3$  section

of dye. This equates to an accumulated pump power of 3.7J, or a full power lifetime of  $0.2\text{Jmm}^{-3}$ . Complete recombination of rhodamine 590 was not however observed.

Output spectra were also taken and they show a consistent blue shift of laser output in sol-gel relative to solution. This is contrary to published work by other authors (10) where a red shift in amplified spontaneous emission was observed.

### **Dye KF 241**

KF 241 is a very convenient dye for sol-gel post doping due to its good solubility in either acetone, ethyl acetate or MMA (methylmethacrylate, the monomer for PMMA). One problem however is KF 241's large size, indicating that only a large pore size sample can be used. Fig 4 shows a comparison of the slope efficiencies of rhodamine 590, pyrromethene 567 and KF 241 solutions under dye laser excitation. The slope efficiency of rhodamine 590 is 13% whilst the slope efficiency of KF 241 in acetone is only 1.3%. The manufacturers of KF 241 (BASF), after being informed of the low efficiency of their dye under microsecond excitation, recommended the use of ethyl acetate to reduce dye aggregation, but with this the slope efficiency of KF 241 in ethyl acetate was still only 3%. Previously published work (2) shows a 9% slope efficiency under nanosecond excitation, so we conclude that KF 241 is very susceptible to triplet state losses, caused by the long microsecond excitation pulses. As a result of the low efficiency, KF 241 has never reached threshold in sol-gel under microsecond excitation.

### **Pyrromethene 567.**

Results when pumped with the flashlamp pumped dye laser are very promising. Fig 4 and table 2 show that a solution in ethanol gave a 14% slope efficiency, better than rhodamine 590 and its threshold in



unindexmatched unpolished sol-gel was only 29mJ per pulse. It gave however only 5 shots of laser action when pumped with 70 mJ per pulse which is an accumulated pump energy of 0.35J and a lifetime of 0.04Jmm<sup>-3</sup>. This is slightly disappointing as a larger lifetime was expected due its unusually low threshold. However due to its low threshold its accumulated output energy, if measured, is expected to be of the same order as with rhodamine 590 in sol-gel/PMMA. It is hoped that PMMA impregnation and polishing will improve the performance and photostability of this dye even further.

### 3.6. Future development

Significant progress is being made in the technical development of solid state dye lasers based on doped sol-gel glass. Further understanding of the underlying science is developing and acts to direct future laser designs. The use of index-matching co-dopants, such as PMMA, has been shown to lead to substantial improvements in optical quality and a reduction in laser threshold.

The directions for further progress are in determining the main reasons for photodegradation of the active dye molecules and implementing designs and active media to optimise the lifetime of the lasers. In a parallel program at Manchester the mechanisms of the dye degradation are under investigation. Processes involving the long lived triplet states and the intrinsic molecular stability are being investigated. The use of the porous sol-gel matrix acting to immobilise and isolate the dye molecules confers added stability.

### 3.7. References.

- (1) T.A.King, D.J.Shaw, C.Whitehurst: SPIE vol.1328(1990)pg183
- (2) R.Reisfeld: SPIE vol. 1328 (sol-gel optics)(1990) pg 29
- (3) J.Ivri, Z.Burshtein, E.Miron, R.Reisfeld, M.Eyal: IEEE J. Quant. Elec.  
26(1990)1516
- (4) M.P.O'Neil: Opt. Lett. 18(1993)37
- (5) T.G.Pavlopoulos, M.Shah, J.H.Boyer: Opt. Comm. 70(1989)425
- (6) J.C.Altman, R.E.Stone, F.Nishida, B.Dunn: SPIE vol. 1758  
(sol-gel optics II)(1992) pg 507
- (7) J.C.Altman, R.E.Stone, F.Nishida, B.Dunn: IEEE Phot. Tech. Lett  
3(1991)189
- (8) L.L.Hench, J.K.West, B.K.Zhu, R.Ochoa: SPIE vol.1328(1990)pg230
- (9) M.Canva, P.Georges, A.Brun, D.Larrue, J.Zarzycki:  
J.Non.Cryst.Solids. 147(1992)636
- (10) D.Lo, J.E.Parris, J.L.Lawless: Appl.Phys.B 56(1993)385

**Table 1. Short pulse length laser results.**

Rhodamine 590	Peak output mJ	Slope efficiency	Wavelength nm	FWHM nm	Photostability Jmm <sup>-3</sup>
Solution	14 (24%)	44%	572	10	/
Sol-gel/PMMA	13 (23%)	26%	572/563*	20	0.67Jmm <sup>-3</sup> #

Pyromethene 567	Peak output mJ	Slope efficiency	Wavelength nm	FWHM nm	Photostability Jmm <sup>-3</sup>
Solution	24 (42%)	43%	560	13	/
Sol-gel	/	20%	559	10	0.13Jmm <sup>-3</sup>

\* Wavelength drift with number of shots.

# Previous best, 0.5Jmm<sup>-3</sup> by B.Dunn at U.C.L.A

**Fig 1. Accumulated pulse energy  
halflives versus pump intensity**

**Halflife (accumulated pulse energy J)**

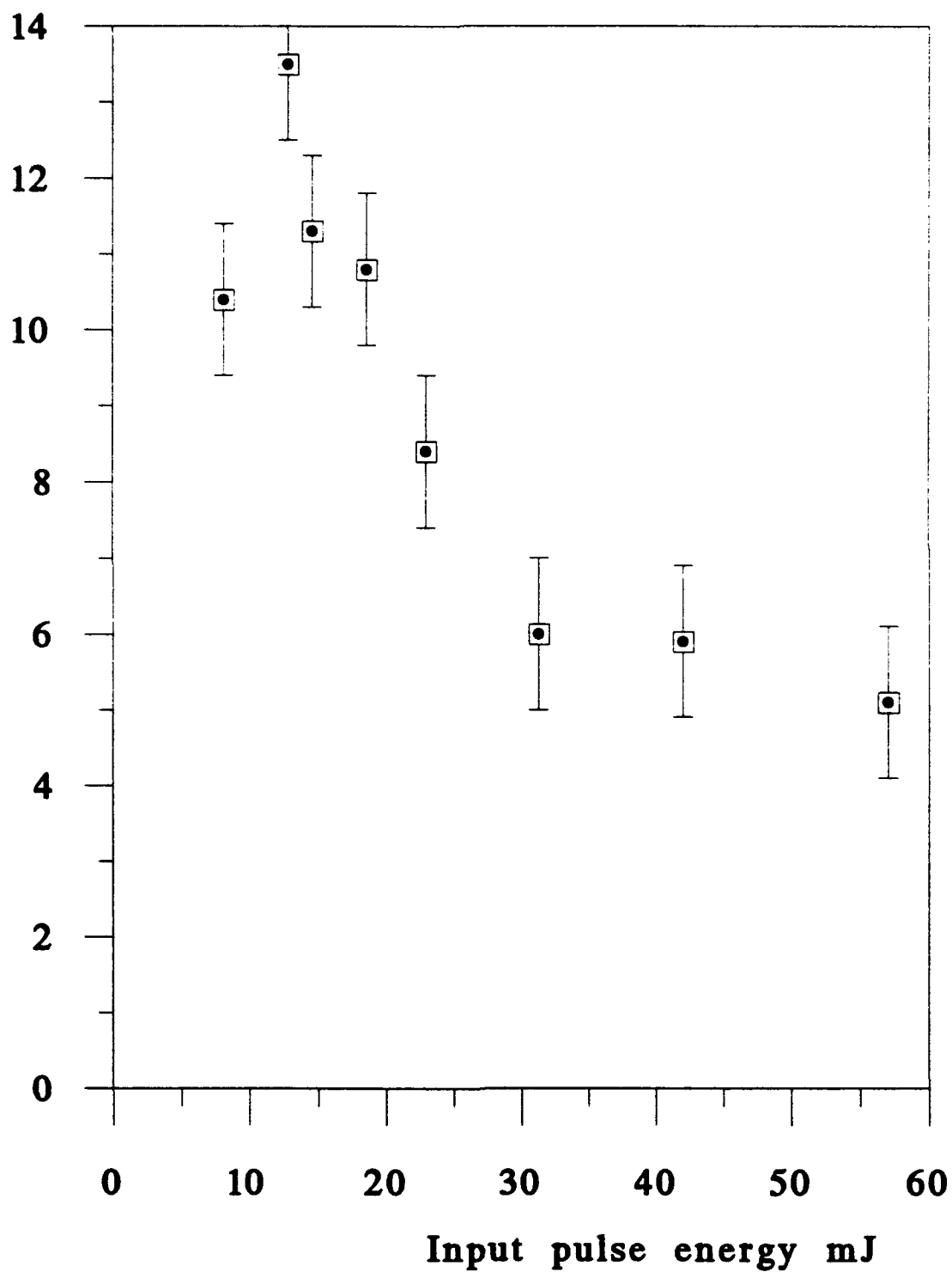


Fig 2. Absorption spectra of rhodamine 590 and  
pyromethene 567

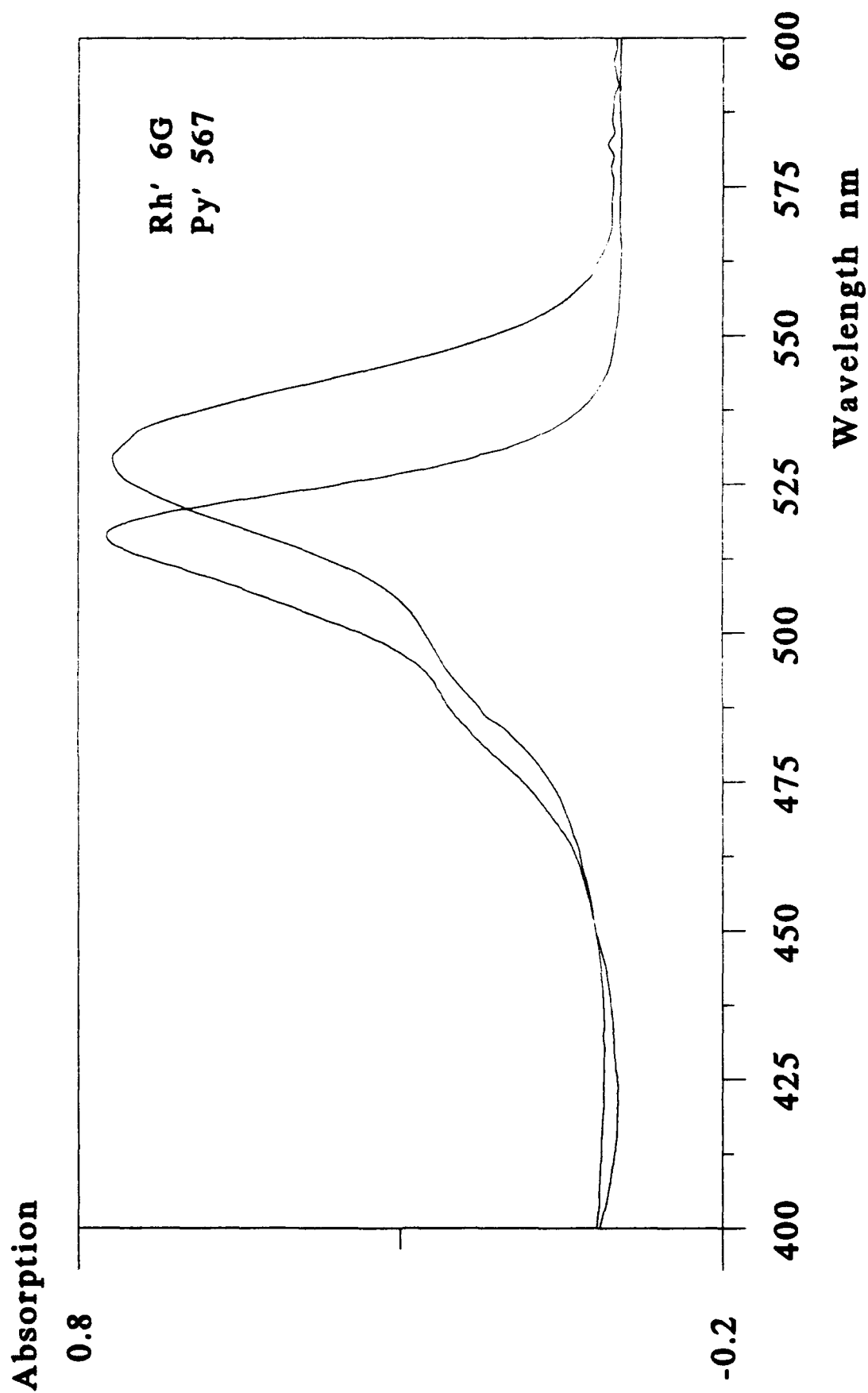


Fig 3. Proposed optimised laser design

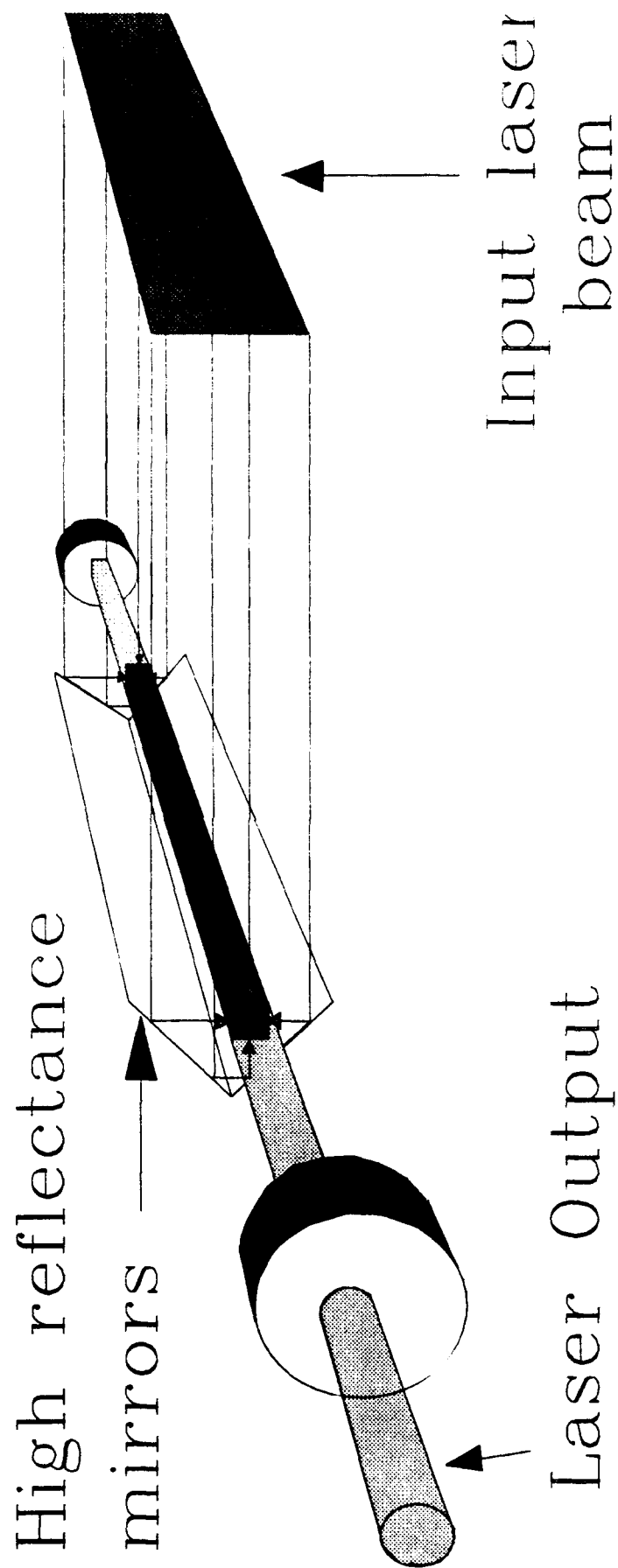
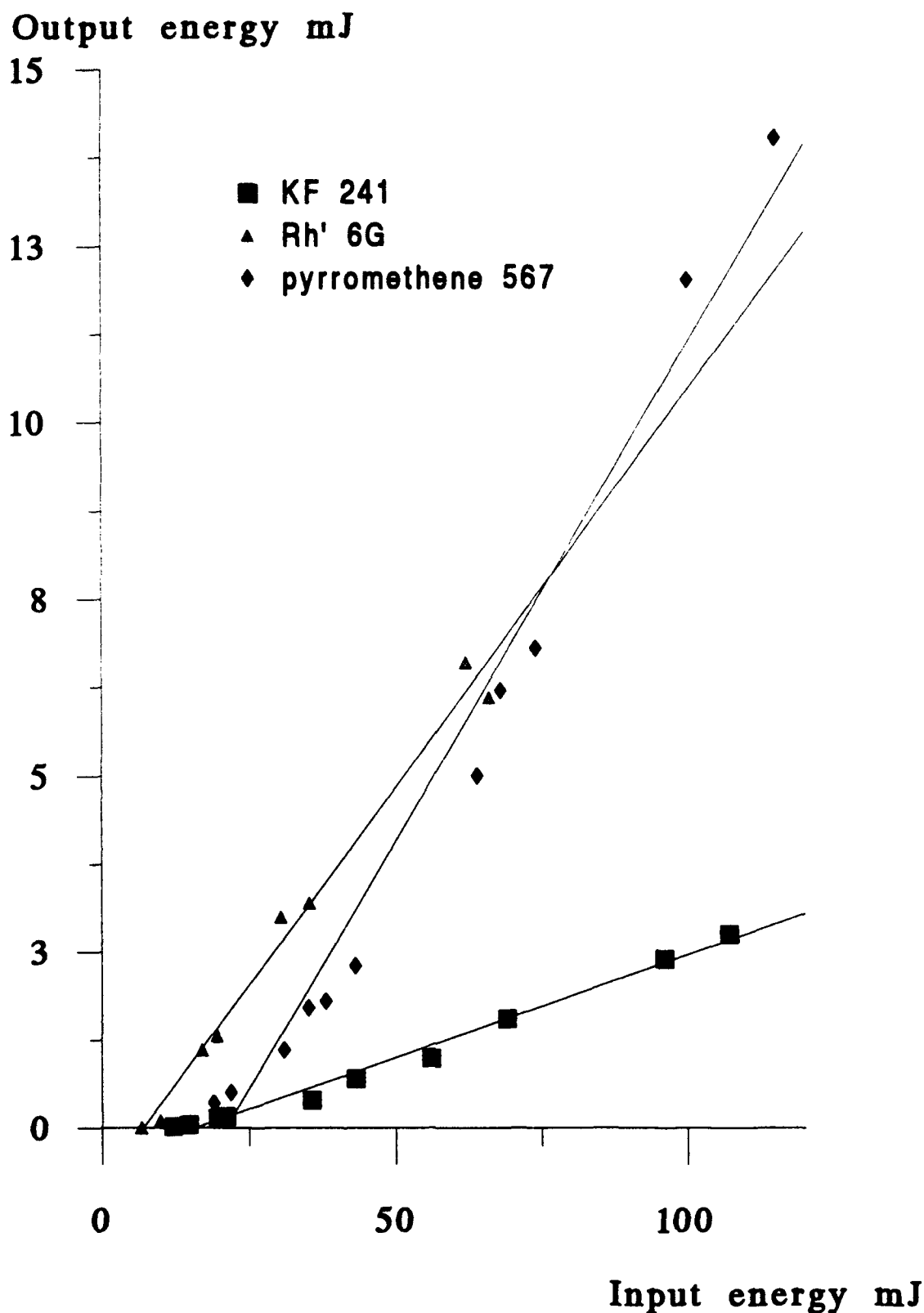


Fig 4. Slope efficiency for KF 241 in ethyl acetate and pyrromethene 567 and rhodamine 590 in ethanol under 3us, 504nm excitation



**Table 2. Long pulse length laser results**

<b><u>Rhodamine 590 under 3μs, 504nm excitation.</u></b>							
	<b>Threshold</b>	<b>Slope efficiency</b>	<b>Beam divergence</b>	<b>Peak output</b>	<b>Full width half max'</b>	<b>Full width</b>	<b>Photostability (Total pump energy) J</b>
<b>Solution</b>	<b>mJ</b> 7*	% 13*	deg .03*	nm 580	nm 12	nm 25	/
<b>Sol-gel</b>	130	/	/	564	6	15	0.03
<b>Sol-gel/PMMA</b>	50	/	/	573	11	28	0.2
<b><u>KF 241 under 3μs, 504nm excitation.</u></b>							
<b>Solution</b>	8*	3*	0.3*	574*	6*	18*	/
<b>Sol-gel</b>	/	/	/	/	/	/	/
<b><u>Pyrromethene 567 under 3μs, 504nm excitation.</u></b>							
<b>Solution</b>	11	14	0.3	/	/	/	/
<b>Sol-gel</b>	29	/	/	549	9	15	0.04

\* These results were taken at the optimum concentration for the dye of  $5 \times 10^{-3}$ M, not  $3.5 \times 10^{-4}$  which was the concentration used for other results.



## **4. Nonlinear Optical Characterisation**

**G. Gall**

### **4.1. Background**

This part of the project is aimed towards the investigation of the properties of sol-gel glasses doped with nonlinear organic materials. Different doping techniques have been investigated and their influence on the linear and nonlinear optical materials are being determined. Comparisons are made between the nonlinear optical properties in solution and in sol-gel glass. It is expected that doped sol-gel glasses would exhibit good optical switching and limiting properties.

Porous sol-gel glasses provide an ideal matrix for hosting optically active organic materials. Sol-gel matrices typically have a porosity of the order of 50%, with approximately 90% of the pores interconnected. The mean pore diameters can range from approximately 1 nm to 20 nm depending on the processing conditions. Consequently the material has a very large effective surface area ( $\sim 500 \text{ m}^2/\text{gram}$ ). This can in certain circumstances lead to enhancement of the nonlinear effects of the dopant due to local field enhancement at the surfaces. The optical transmission of silica sol-gel glass is from the UV to the IR with a transmission similar or better than fused silica.

The optical quality and scatter in sol-gel glasses depends on the pore size and distribution, and the best optical quality is generally obtained for smaller pore sizes. Hence it is important to select the smallest pore sizes which allow proper doping of the particular dopant of interest. This optimum pore size will depend on the shape and size of the molecules and also on any interactions between the molecules and the sol-gel matrix. The optimum pore size can be assessed by measuring the penetration depth of the dopant from a solution in sol-gel samples of different mean pore sizes. This is achieved by using the laser induced fluorescence technique described in earlier reports.

The large nonlinear coefficients of certain organic materials together with the high doping concentrations achievable in sol-gel make optical switching and limiting feasible in relatively thin films. These can be prepared by spin-coating the sol-gel material onto a substrate. In this case the organic nonlinear material can be doped into the sol-gel either prior to the spin-coating or by post-doping from a solution.

Nonlinear optics is becoming increasingly important in many fields such as the communications industry. Devices with high optical nonlinearity and extremely fast response times, ps-fs, are being sought which would enable rapid transfer of data via optical links. Using optical analogues of currently available semiconductor technology, optical supercomputing would become a reality. To this end components which show high nonlinearity, fast response times, high laser damage thresholds and relative ease of production are extremely desirable.

#### **4.2. Experimental Program**

Two families of dyes which show high nonlinear optical coefficients have been chosen for impregnation into sol-gel derived materials. Dithiolene derivatives and phthalocyanine (Pc) derivatives have been post-doped into polished xerogels, and pre-doped into Ormosil host material which provide both a physically and chemically stable environment for the nonlinear species. The phthalocyanine dyes show particular promise in the field of Optical Limiting, which occurs due to the process of reverse saturable absorption. Listed in Table 1 are recent experimental results of both the phthalocyanine and dithiolene dyes.

Xerogel samples were obtained from Geltech, Florida, U.S.A., in the form of discs roughly 30mm in diameter and 6mm thick. Absorption spectroscopy using a Perkin Elmer lambda 9 spectrophotometer has shown that these xerogel samples have excellent transmission properties from ~300nm-1500nm. Forward scatter/attenuation measurements performed at Manchester using the experimental arrangement shown in Figure 4.1 indicate low linear losses of <1.0dB/cm, which is suitable for

device manufacture. Figure 4.2 shows the forward scatter of an 800°C 50Å mean pore diameter sample, code SM 93-3502-6-6.

Using a Logitech diamond wire saw, rectangular samples of roughly 6x3x30mm were obtained. This technique allows several samples to be acquired from one bulk, which can then be used for different characterisation experiments. The 'wafer' samples were then optically polished using a Logitech PS2000 polishing system, which can allow surface flatness of  $\lambda/10$  to be achieved repeatably.

Polished xerogel samples were immersed in solutions of the optical species of interest. These samples were left for 7 days at 40° to allow for homogenous diffusion of the dye through the xerogel. After 7 days the samples were removed and dried under vacuo to remove all traces of solvent. For the ormosil samples, the nonlinear species was added at the sol-stage. After ageing and drying these samples were then optically polished using 3µm diamond paste.

Preliminary results suggest that a sample thickness of 2-3mm, and a dopant concentration of  $10^{18}$  molecules/cm<sup>3</sup> yield good nonlinear optical coefficients. Effects of dye concentration are currently being explored.

$\chi_{xxxx}^{(3)}$  coefficients were investigated using a retro-reflection degenerate four wave mixing technique. 100ps pulses were selected from a Q-switched mode-locked Quantel Nd:YAG with a final beam diameter of 300µm. The pump and probe beams were separated by 3.5°, and the phase conjugate beam sampled by a 50% beam splitter in the probe beam's path. All signals were logged from silicon photo detectors into a boxcar, and the results were calibrated using

CS<sub>2</sub> :  $\chi_{xxxx}^{(3)} = 2.5 \times 10^{-20} \text{m}^2/\text{V}^2$ . The use of a half wave plate in the pump beam allows the mechanisms for the nonlinearity to be determined.

Initial results for the dithiolenes suggest similar  $\chi^3$  values to those of the doped PMMA host (see Table 1). However, the excellent transmission properties and larger optical damage thresholds of the sol-gel host media, coupled with the ease of preparation of the doped composites offer attractive advantages over the polymer host.

Z-scan measurements of a CAP doped xerogel were obtained using an experimental arrangement as shown in Figure 4.3. A 15ns doubled Nd:YAG with a 1/e diameter of 7 $\mu$ m in a high quality TEM<sub>00</sub> Gaussian beam was used in a tight focus geometry. The transmittance of the sample was then measured through a 40% aperture as a function of the sample position z measured with respect to the focal plane. Figure 4.4 shows what is believed to be the first Z-scan result obtained on a post-doped xerogel. The 'dip' in the graph shows the characteristic shape of a nonlinearly refractive material. Future improvements in the experimental set-up will allow precise nonlinear coefficients to be obtained with this method, which can then be compared to those generated by the DFWM technique.

THG has been performed using the Maker fringe technique, preliminary results suggest that the nonlinear coefficients are of a similar order of magnitude to those quoted in Table 1, and are due to a real electronic effect. Currently an Optical limiting experiment is being commissioned which will allow optical limiting, Z-scan and laser damage measurements to be performed.

Table 1

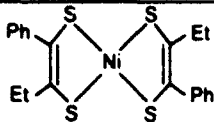
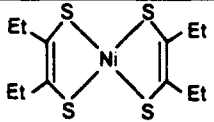
Author/Journal	Dopant	Host	Experiments performed	Results
C.S. Winter J.Appl.Phys 71 (1) 1992		PMMA	D.F.W.M. Damage	$\chi^3: 10^{-17} \text{m}^2/\text{V}^2$ $> 1 \text{GW}/\text{cm}^2$
C.S. Winter J.Mats.Chem. 1992	13 dithiolene compounds	PMMA	D.F.W.M. Z-scan	$\chi^3: 10^{-20} \text{m}^2/\text{V}^2$
C.S. Winter Organic Materials for NLO & Photonics 383-90, 1991	dithiolate compounds	solution	D.F.W.M. linear absorption	$\chi^3: 10^{-18} \text{m}^2/\text{V}^2$ $\alpha: 0.1 \rightarrow 22 \text{cm}^{-1}$
C.S. Winter Appl.Phys.Lett 52,2,1991 pp107-9		solution	D.F.W.M. linear/two photon absorption	$\chi^3: 10^{-20} \text{m}^2/\text{V}^2$
T. Fukawa SPIE 1626 pp.135-9 1992	Ni(dmbit) <sub>2</sub> TBA	solution	THG	$\chi^3: 7 \times 10^{-14} \text{esu}$
Z.H. Kafafi SPIE 1626, 1992 p.440-9,	Benzenedithiol O-Amino B.D.T.	solution	D.F.W.M. time resolved	$\chi^3: 10^{-11} \text{esu}$
D.R. Coulter SPIE 1105 p.42-51, 1989	CAP, PC's and NPC's	solution	Optical Limiting	60 $\mu\text{J}$ limiting throughput
P.D. Fuqua SPIE 1758 p.499-506, 1992	GePc, CuPc4S, SnPc	sol-gel (pre- doped)	Optical Limiting	0.1 $\mu\text{J}$ threshold
N.Q. Wang SPIE 1328 p.100-7 1990	SINC	sol-gel (pre- doped)	THG	$n_2: 10^{-4} \text{cm}^2/\text{kW}$
J.W. Perry Organic Materials for NLO & Photonics, pp369-382, 1991	CAP SINC	solution	Optical Limiting, ps & ns Nonlinear Absorption	1.6 $\mu\text{J}$ threshold

Figure 4.1 Forward Scatter/Attenuation experiment

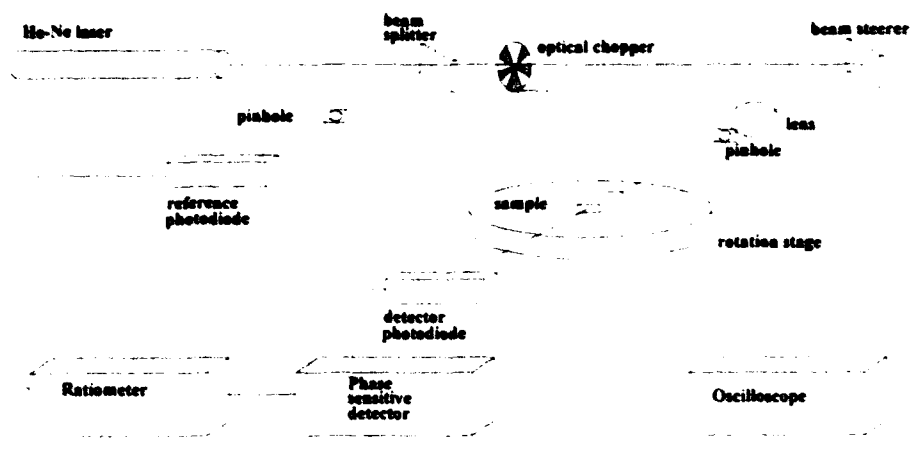


Figure 4.2. Forward scatter results on 800°C 50Å xerogel.

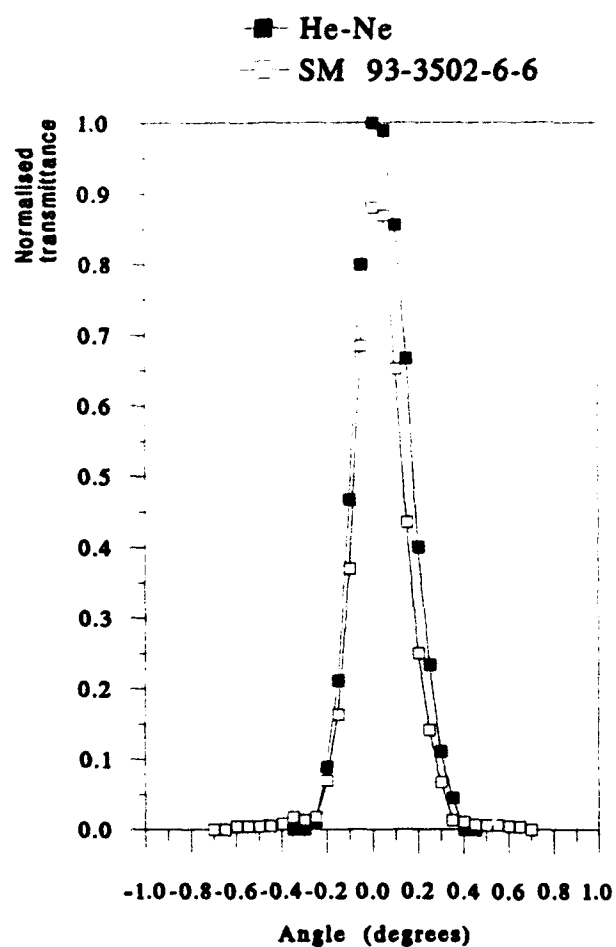


Figure 4.3

### Z-scan experimental arrangement

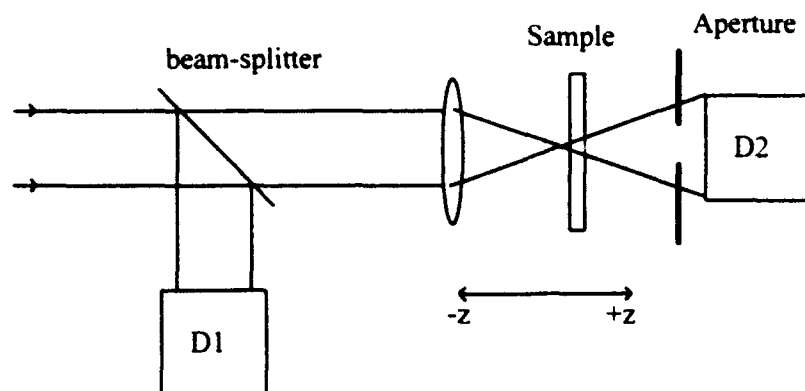
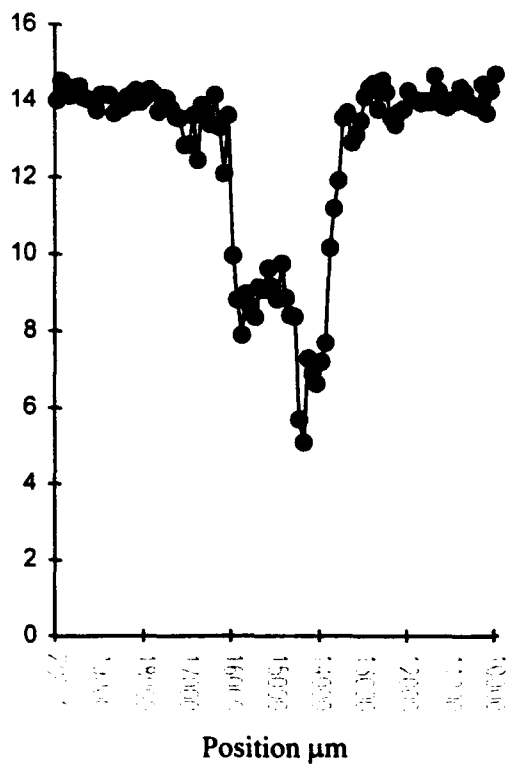


Figure 4.4. Z-scan result of CAP doped xerogel.

Transmitted signal (arb)



## References

P.A. Miles, "Material figures of merit for saturated excited state absorptive limiters", OE Lase'94, LA. CA. USA, 22-29 Jan 1994.

D.J. Harter, M.L. Shand, Y.B. Band, "Power/Energy limiter using reverse saturable absorption", J.Appl.Phys **56** (3) 1984.

J.S. Shirk, J. R. Lindle, F.J. Bartoli, Z.H. Kafafi, A.W. Snow, M.E. Boyle, "Third-order nonlinear optical properties of metallo-phthalocyanines", Int.J.Nonlinear Optical Physics, **1**, 4, 1992, 699-726

K. Mansour, D. Alvarez Jr; K.J. Perry, I. Choong, S.R. Marder, J.W. Perry, "Dynamics of optical limiting in heavy-atom substituted phthalocyanines", SPIE 1853, 1993 pp132-141

S.W. McCahon, L.W. Tutt, M.B. Klein, G.C. Valley, "Optical limiting with reverse saturable absorbers", SPIE 1307, 1990 pp.304-314